Chapter-4

Results and Discussion.

In this chapter, the results obtained from different techniques showing the fluence dependent modifications induced in the polymers by Li-ion irradiation have been discussed in terms of structural, electrical, thermal and mechanical properties. Application of ion beam modified polymer in gas sensor has also been discussed.

Chapter 4

Results and Discussion

Chapter–4

Results and Discussion

In this chapter the results derived from all the experiments described earlier in chapter 3 for pristine and irradiated samples are presented. The effect of irradiation on the physico-chemical properties of all polymers is reported. Structural analysis was studied by FTIR Spectroscopy. The electrical properties were measured using an LCR meter. AC conductivity, dielectric loss (tan δ) and dielectric constant were measured as a function of temperature and frequency. Thermal stability was studied by Thermogravimetric analysis (TGA). Mechanical property (microhardness) was analysed by Vicker's microhardness indenter. Tensile strength was measured by Instron Tensile tester.

This chapter is divided into five parts to explain the results of five polymeric materials separately and exclusively. The selected polymers for the work of this thesis are PP, PET, PI, Blend of PVC & PET, and Blend of PVC & EVA.

4.1. Polypropylene

As discussed in chapter 3 (article 3.2.1) Polypropylene belongs to the family of polyolefin. It is a vinyl polymer having hydrogen atom substituents, $(-H_2C-CH_2-)_n$ and undergoes dominant homolithic rupture of C-H bonds to form hydrogen free radicals, which cross-link with each other. Polypropylene is a transparent, soft and thermoplastic polymer. Being highly crystalline, it exhibits high stiffness, hardness and tensile

strength. Polypropylene is an important engineering polymer because of its several advantages in cost and performance. For health care and packaging applications PP has the advantage of being nontoxic and inert to liquids and drugs. PP is used as a capacitor dielectric because of its very low dielectric loss and excellent dielectric strength.

Polymers having conductivities above the semiconductor range have been produced by chemical doping. The increased conductivity achieved by the addition of dopants can be unstable, and may decrease with the loss of dopant. The advantage of ion irradiation over chemical doping lies in the fact that irradiation can utilize additives that cannot be applied chemically because of their low volatility and/or insolubility in suitable solvents. Chemically doped conducting polymers have a problem of thermal instability. KeV and MeV ion irradiation on polypropylene has been reported in the past.

Wang et al [1], studied the effects of 100KeV proton irradiation on polypropylene, which leads to cross-linking between the macromolecules of the polymer and enhances its mechanical properties. Optical and electrical properties of 2MeV electron and 62 MeV proton irradiated polymers (i.e. PTFE, PI, PET and PP) have been reported by Mishra et al [2]. The shift in optical absorption edges as observed by UV VIS spectra of the irradiated polymer has been correlated to the optical band gap using Tau's expression. A decrease in the optical band gap has been observed in irradiated PP and PTFE. AC conductivity measurements confirmed an increase in conductivity due to electron irradiation of PP.

Mishra et al [3] studied the effects of 2MeV electron irradiation on polypropylene by different characterization techniques like, FTIR spectroscopy, electron spin resonance spectroscopy, thermogravimetry analysis, differential scanning calorimetry and X-ray diffraction analysis. The thermal stability of the polymer was found to be increasing due to electron irradiation. The isotactic nature of the polymer was found to be unaffected by electron irradiation. An increase in crystallinity of the polymer has also been observed after irradiation.

But the detailed study of dielectric properties at different temperature and frequency has not been reported so far.

In the present work, the effect of 50 MeV Li^{3+} ion irradiation on polypropylene (PP), has been studied at different fluences. The modification in electrical properties (resistivity/conductivity, dielectric loss and dielectric constant) has been studied by variable frequency LCR meter. Resistance, tan δ and capacitance were measured at different frequencies ranging from 0.05 to 100 KHz and temperatures ranging between ambient temperature (40°C) to 140°C respectively [4,5].

4.1.1   Structural Analysis.

The change in chemical structure of polypropylene due to ion irradiation is identified by FTIR spectroscopy. The IR spectra of pristine and irradiated PP films are shown in **Figure 4.1.** The most important change with higher fluence (1.5 x 10^{14} ions/cm^2) occurs at ~2900 cm^{-1}. This particular wave number is associated with C-H stretching. The decrease in intensity at this point indicates that the C-H bond is affected to some extent probably because of breaking of some of the bonds.

The main effect of irradiation is the formation of new bonds, free radicals, double bonds etc. PP has saturated bonding. The irradiation is expected to give rise to C=C observed in 1680-1620 cm^{-1} region. It is seen that some absorbance occurs around this region. Moreover, there is some absorption at 1671 cm^{-1} even for pristine sample, which could be due to the presence of unsaturation. After a fluence of 3.4 x 10^{13} ions/cm^2, the absorbance is observed at 1450 cm^{-1} which is also seen at the fluence of 2.4 x 10^{12}, or 1.5 x 10^{14} ions/ cm^2 as well as in the pristine sample. This may be due to the fact that the C-H bonding does not get affected due to irradiation, whatever the fluence may be i.e. the nature and characteristic of C-H bond does not change. The spectra has many absorbance over the whole range and some of them are difficult to decipher. The presence of alkene and alkyne groups in pristine sample seem to get modified by irradiation and can be noted by the change in the position and intensity of absorbance in the ~630 to 900 cm^{-1} region. The irradiation also affects the polymer by forming carbonaceous materials which could also be observed by the naked eye. The IR spectra indicate the formation of such material. Moreover, the interaction between the H of PP with oxygen from air may also be possibly making the IR spectra reasonably complicated. Some indication of it can be found in the presence of absorbance at the 3500 cm^{-1} region. The 984 cm^{-1} band is not much affected by irradiation though 1168 cm^{-1} band is affected showing that 3/1 helix structure gets somewhat affected by Li^{3+} irradiation though electron induced irradiation does not do so [3].
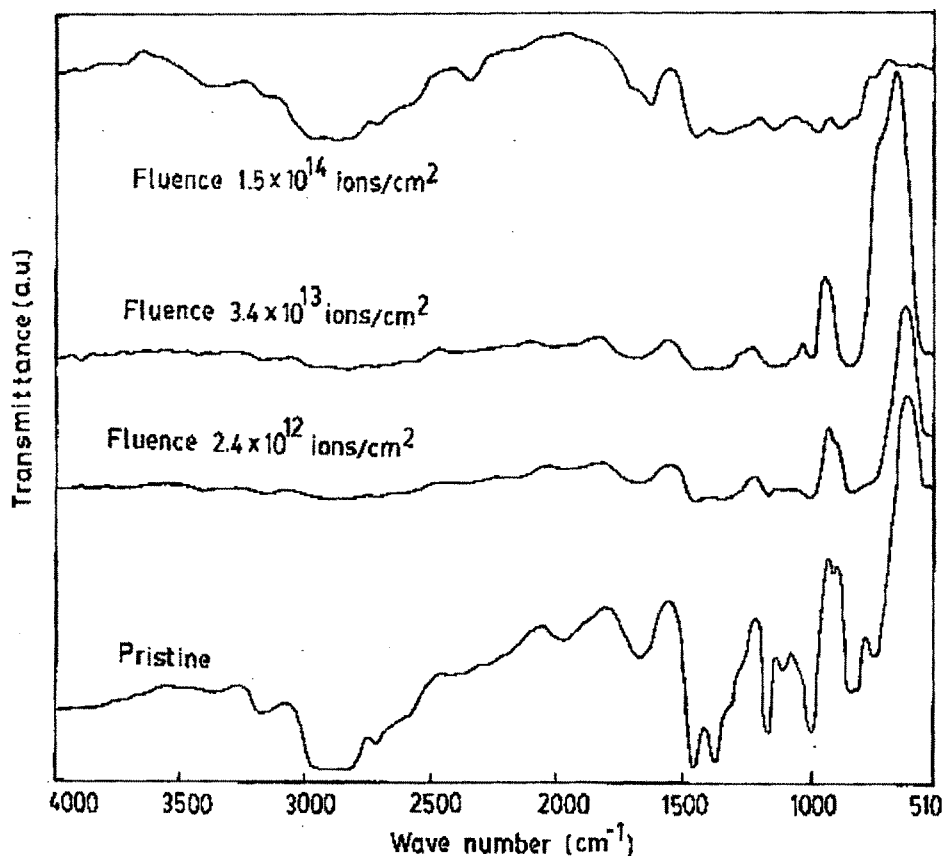
Figure 4.1   **FTIR spectra of pristine and irradiated PP samples.**

4.1.2   Electrical Properties of Polypropylene

Electrical properties of pristine and irradiated PP samples were measured using an LCR meter. The frequency was varied from 0.05 to 100KHz, while the temperature was varied from ambient to 140°C respectively. Resistivity and conductivity were calculated using the formula given by equations (2.4) and (2.5) in article 2.3.1 (c) of chapter 2. The dielectric constant was calculated using the formula given by equation (2.9) in

article 2.3.1 (d) of chapter 2. The findings with their respective explanation are as follows.

4.1.2 (a) log Resistivity v/s log Frequency

From **Figure 4.2** it is observed that the resistivity decreases rapidly in proportion to f^{-1}. The resistivity also decreases as the temperature increases.

An ac field of sufficiently high frequency applied to a metal polymer metal structure may cause a net polarization, which is out of phase with the field. This results in ac conductivity, it appears at a frequency greater than that at which traps are filled or emptied [6].

From the **Figure 4.3** it can be seen that the resistivity of PP samples decreases as frequency increases. It can also be seen that resistivity decreases with increase in fluence.
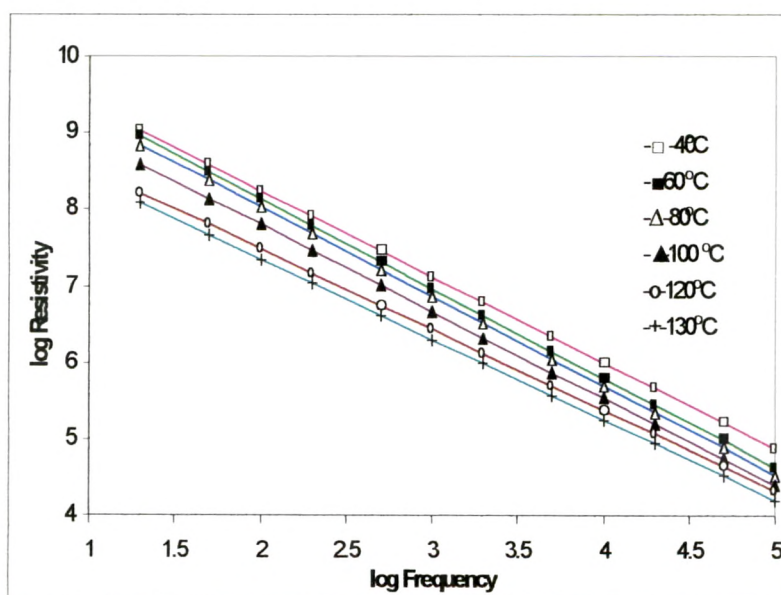

Figure 4.2   **Plot of log Resistivity v/s log Frequency (f in Hz) at different Temperatures (°C), keeping fluence (1.5 x 10^{14} ions/cm^2) constant.**
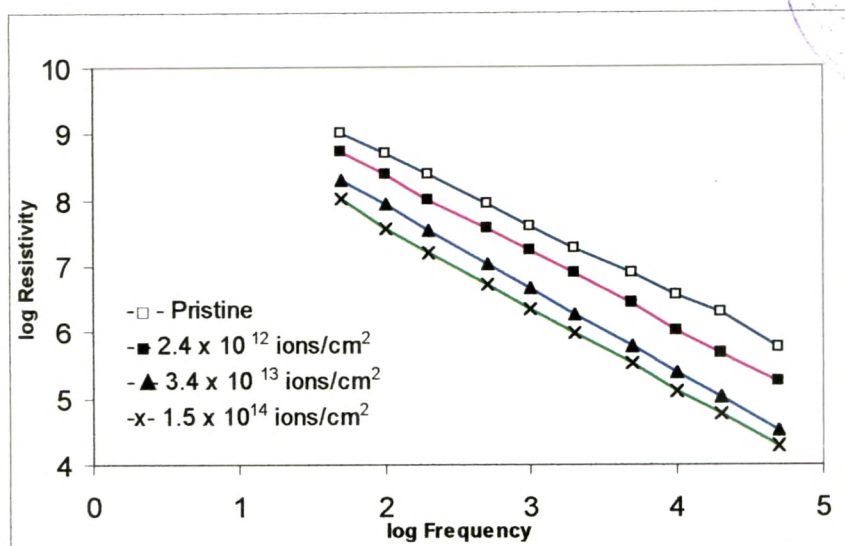
Figure 4.3   Plot of log Resistivity v/s log Frequency (f in Hz) at different fluence keeping temperature constant

4.1.2 (b) Conductivity v/s log Frequency

Figure 4.4 shows the dependence of conductivity, (inverse of resistivity) of PP films on log frequency (f in Hz) at ambient temperature for pristine and irradiated samples. A sharp increase in conductivity has been observed at 20 kHz. It is also observed that conductivity increases as fluence increases. The increase in conductivity due to irradiation may be attributed to scissioning of polymer chains and as a result, increase of free radicals, unsaturation etc. When an a.c. field of sufficiently high frequency is applied to a metal polymer metal structure, it may cause a net polarization, which is out of phase with the field. This results in a.c. conductivity, it appears at frequency greater than that at which traps are filled or emptied [6,7].
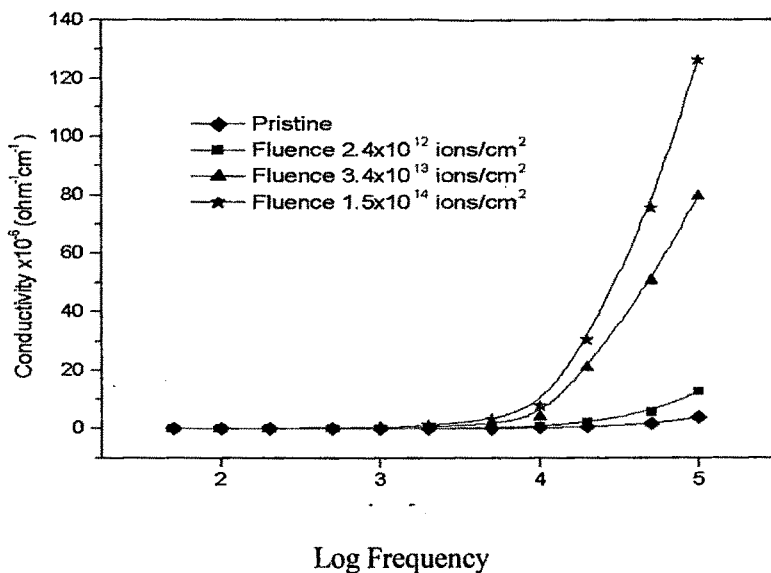
Figure 4.4   **Plot of Conductivity v/s log Frequency (f in Hz) for pristine and irradiated PP samples at ambient temperatures.**

4.1.2 (c)   tanδ v/s Temperature

Figure 4.5 shows the behaviour of dielectric loss (tan δ) versus temperature at a frequency of   10 kHz for pristine and irradiated samples. It can be seen that all PP samples show two relaxation peaks at 60°C and 120°C respectively. The small and activated phenomenon at low temperature (60°C) is due to the local motion of pieces of the polymer backbone in agreement with the observations of Wintersgill and Fontanella 1989 [8], while the large peak is due to the heat distortion (or heat deflection) temperature (HDT) at 120° C. In the case of an amorphous polymer, HDT is slightly (10 to 20°C) lower than the T_g as determined by thermal techniques, while in the case of semicrystalline polymers, HDT is more closely identified with T_m [9] .HDT is a useful indicator of the temperature limit above which polymers can not be used for

structural (load-supporting) applications. It is observed from the tan δ vs temperature plot that maximum in dielectric loss (tan δ) at a particular temperature is independent of the fluence. The value of tan δ is also found to increase with increasing the fluence. The dielectric loss is due to the perturbation of the phonon system by an electric field, the energy transferred to the phonons being dissipated in the form of heat.

Figure 4.6 shows the variation in tan δ with temperature at different frequency keeping fluence constant. The dielectric loss is due to the perturbation of the phonon system by an electric field, the energy transferred to the phonons dissipated in the form of heat. PP is a non-polar material, so orientational polarization cannot assume a major portion. Non polar materials contain a small number of free charge carriers and charge migration is usually investigated as an activated diffusion process, in which the carrier jump from one position to another, each time surmounting an energy barrier, which could be due to interfaces between the crystalline and amorphous region of the polymer. Moreover, due to arbitrary chain arrangements in the amorphous region of the polymer, the Vander-Waals forces differ from place to place. On the other hand in the crystalline areas, because of the presence of hindering structural units (due to greater density of these regions) the polymeric chains move with a greater difficulty than in the amorphous regions. This hindrance can be assumed to posses a certain potential energy, when the polymer is heated the movement of the large segments of the main chain sets in and becomes maximum [10].
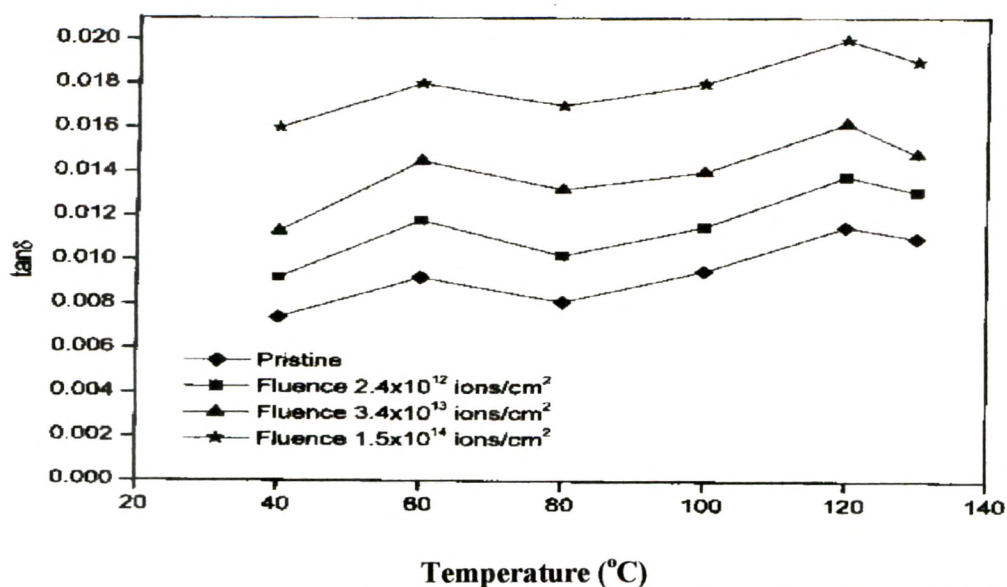
**Figure 4.5**　　　　Plot of Dissipation factor (tanδ) v/s Temperature (°C) for

pristine and irradiated PP samples at 10 kHz frequency.
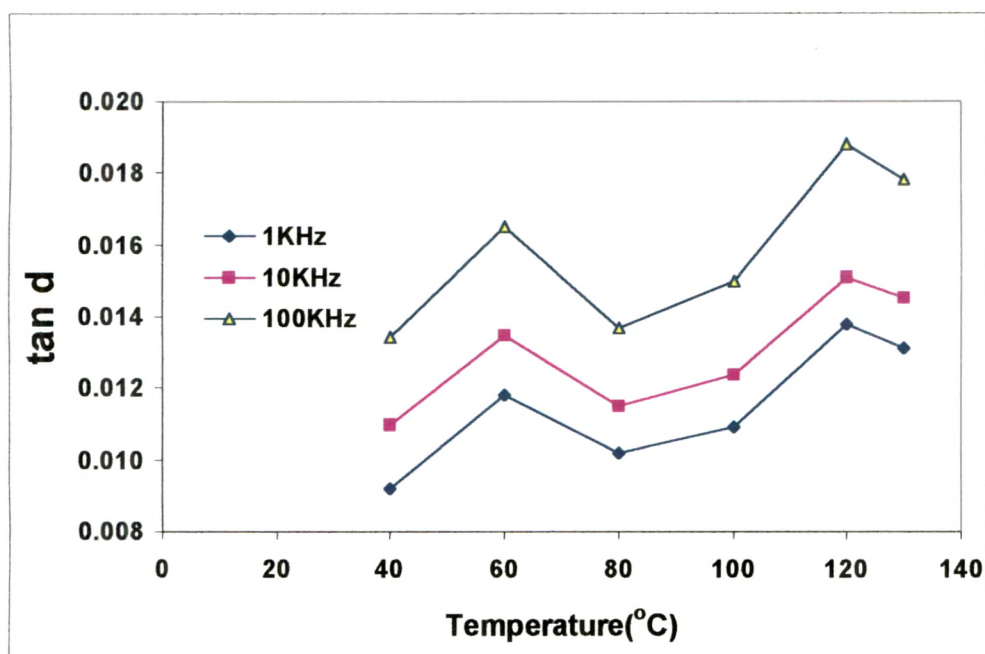
**Figure 4.6**　　　　Plot of Dissipation factor (tan δ) v/s Temperature (°C) at

different Frequency keeping fluence (1.5x10^{14}ions/cm^{2})

constant.

4.1.2 (d) tan δ v/s log Frequency

Figure 4.7 shows the behaviour of tan δ measured as a function of frequency at different temperatures keeping fluence constant $(1.5 \times 10^{14}\, \text{ions/cm}^2)$. It is observed that with the increase in frequency, dielectric loss (tan δ) shows moderate increase up to 10 kHz at all temperatures, suggesting that PP films can be used as dielectrics in capacitors being used below 10 kHz frequency.

Figure 4.8 shows the behavior of dielectric loss (loss factor) with the increase of frequency at different fluences, at ambient temperature. It is observed that loss factor increases moderately as frequency increases. It is also observed that the loss factor increases as fluence increases. The growth in tanδ and thus increase in conductivity is brought about by an increase in the conduction of residual current and the conduction of the absorption current [7].
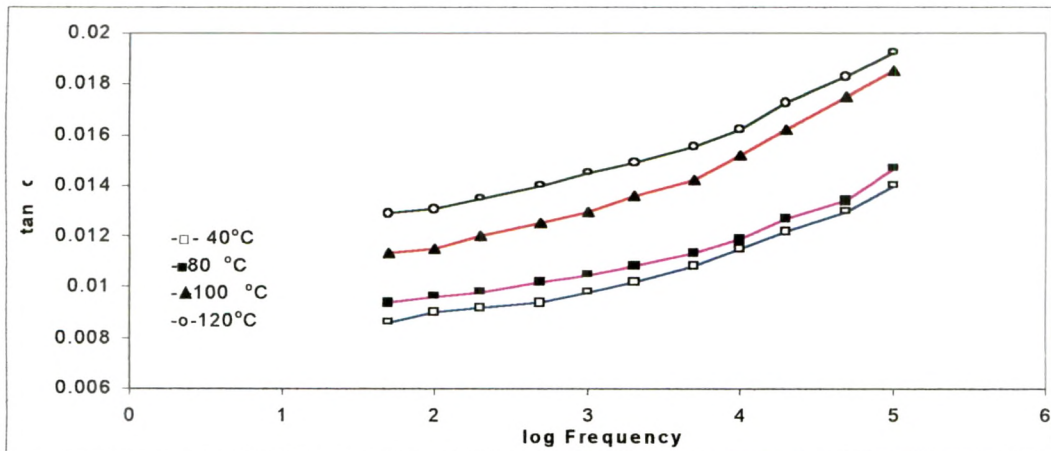

Figure 4.7   Plot of Dissipation factor (tan δ) v/s log Frequency (f in Hz) at different temperatures (°C), keeping fluence $(1.5 \times 10^{14}\, \text{ions/cm}^2)$ constant.
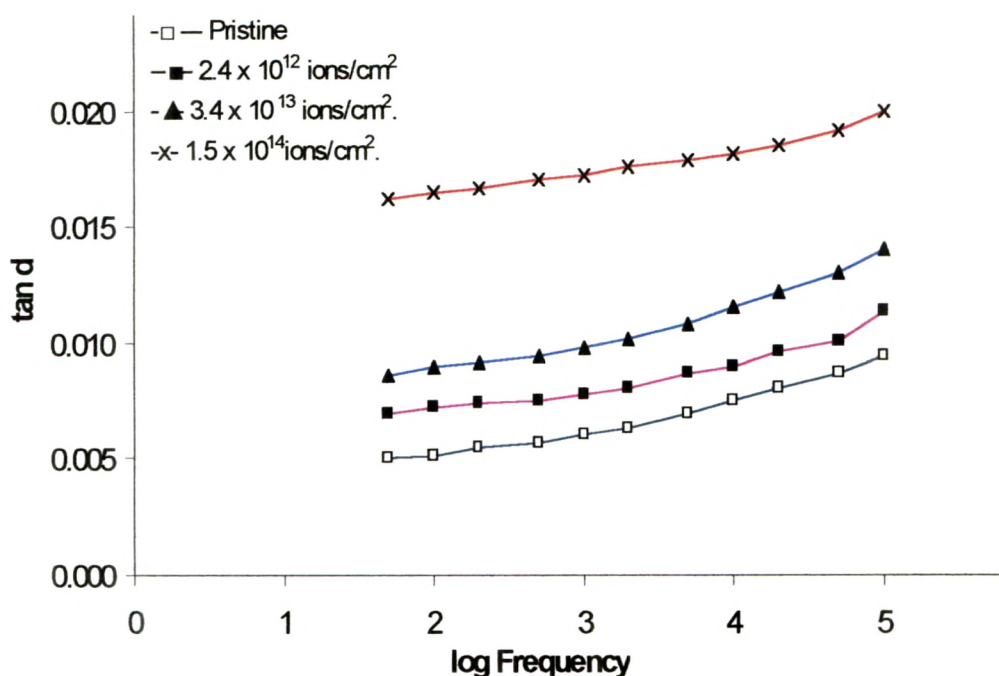
Figure 4.8   Plot of Dissipation factor (tanδ) v/s log Frequency (f in Hz) at different fluence at ambient temperature.

4.1.2 (e) Dielectric Constant v/s log Frequency

The capacitance of the sample was measured using an LCR meter as described in chapter 3 (article 3.2.2) and from that the dielectric constant of the film (sample) was calculated using equation (2.9) in chapter 2. The results obtained are graphically shown in figures 4.9 and 4.10 respectively.

Figure 4.9 shows the behavior of the dielectric constant as a function of frequency at different fluences $(2.4 \times 10^{12} - 1.5 \times 10^{14}$ ions/cm^2) for Ag-PP-Ag structure. It is observed that the dielectric constant remains constant in the frequency range $0.05 - 100$ kHz. At these frequencies the mobility of the free charge carrier is constant and thus the dielectric constant is constant [11]. It is also observed that dielectric constant increases

as ion fluence increases. The increase in dielectric constant may be attributed to the chain scission and as a result the increase in the number of free radicals etc. It is an interesting observation because a lot of PP based capacitors are used in nuclear plants and are bound to be exposed to nuclear radiation.
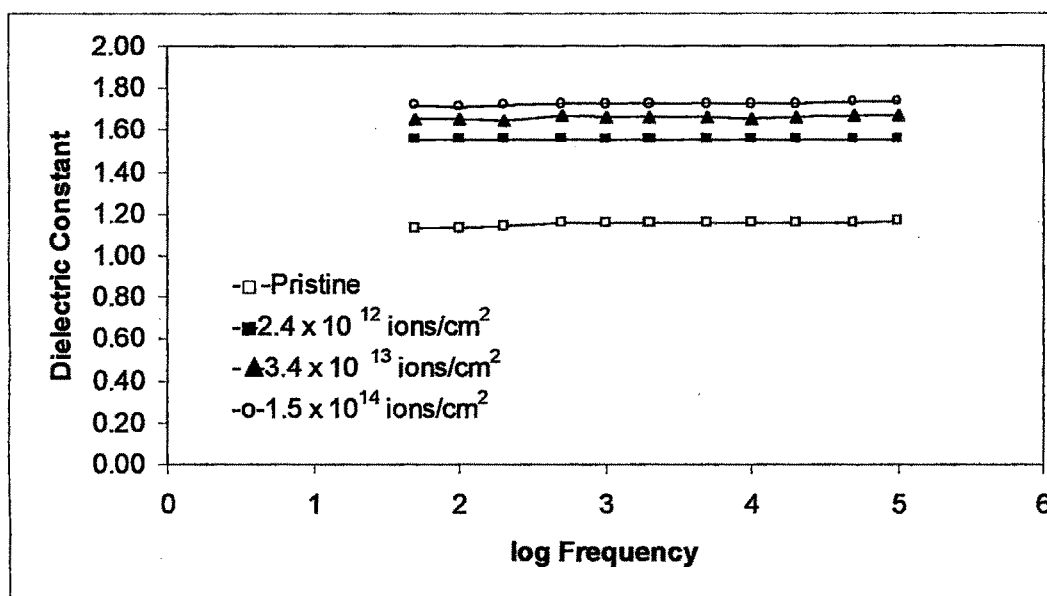
Figure 4.9   Plot of Dielectric Constant v/s Log Frequency (f in Hz) at different fluences.

4.1.2 (f)   Dielectric Constant v/s Temperature

Figure 4.10 shows dielectric constant as a function of temperature at constant frequency of 10kHz for pristine and irradiated samples. Dielectric constant is almost independent of temperature. The negligible change (~6%) with temperature could be due to the effect of conductance corresponding to absorption current. It is also observed that dielectric constant increases with the increase in fluence. This increase in dielectric

constant may be attributed to the chain scission which results in an increase in the number of free radicles etc.
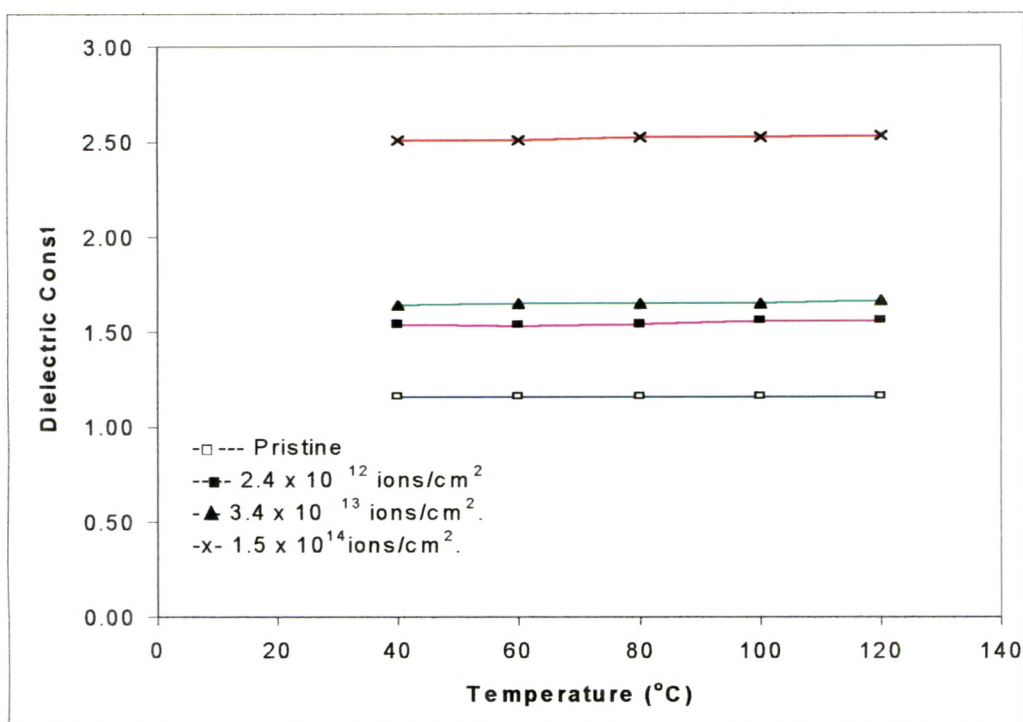
Figure 4.10 Plot of Dielectric Constant v/s Temperature(^{o}C) at different fluences.

4.1.3 Thermal Analysis of Polypropylene (Thermogravimetric analysis)

The decomposition behaviour of the pristine and irradiated (at the fluence of 1.5×10^{14} ions/cm^2) polymers was examined by this technique. The thermograms are as shown in the **Figure 4.11**. The results obtained are shown in **Table 4.1**. As seen in the figure the stable zone appeared for the irradiated polymer up to 80°C, which was up to

210°C for pristine PP. The slow decomposition zone was up to 260°C for pristine, which was up to 180°C for irradiated sample, involving only about 19% weight loss for the pristine, whereas a weight of about 5% was lost in case of the irradiated sample. Similarly, the fast decomposition zone went up to 320°C involving a weight loss of about 67% for the pristine and up to 400°C for the irradiated polymers associated with a weight loss of about 70%. From the data, it is observed that the decomposition nature of the polymer varied due to ion beam irradiation. The irradiated film decomposed earlier compared to the temperature at which decomposition of pristine polymer started. This denotes a degradation of the polymer matrix under Li^{3+} ion irradiation.
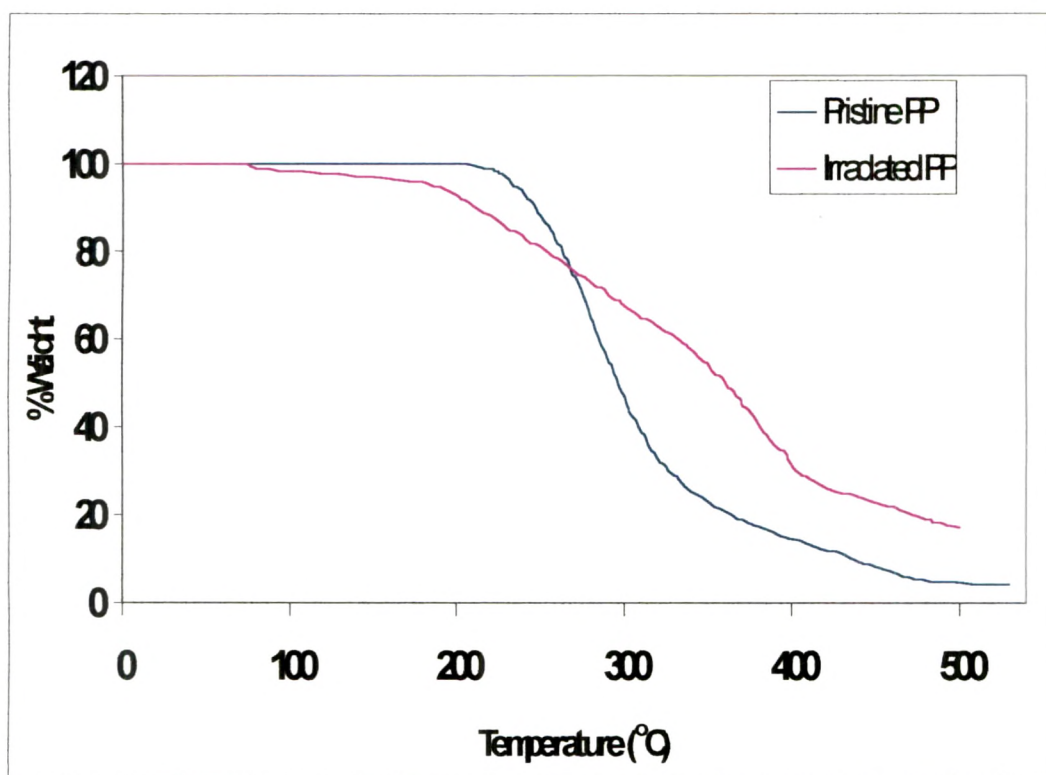

Figure 4.11   TGA thermograms of pristine and irradiated PP

Table 4.1   **Data derived from TGA thermogram of pristine and irradiated PP denoting their thermal decomposition behaviour.**

Sample Weight (mg)	Zone	Temperature Range	Weight loss (%) in zone	Total Weight loss (%)	Remark
Pristine	I	0°C to 210°C	0	0	Stable Zone
	II	210°C to 260°C	19	19	Slow Decomposition
	III	260°C to 320°C	48	67	Fast Decomposition
	IV	320°C to 520°C	28	95	Residue
Irradiated	I	0°C to 80°C	0	0	Stable Zone
	II	80°C to 180°C	5	5	Slow Decomposition
	III	180°C to 400°C	65	70	Fast Decomposition
	IV	400°C to 500°C	12	82	Residue

4.1.4   Conclusion

The FTIR spectra showed a decrease in intensity of 2900 cm^{-1} peak, which is associated with stretching vibrations of C-H bond. The main effect of irradiation is the formation of new bonds, free radicals, double bonds etc. The irradiation is expected to give rise to C=C bond observed in the 1680 − 1620 cm^{-1} region. The 984cm^{-1} bond is not much affected by irradiation though the 1168cm^{-1} bond is affected showing that the 3/1 helix structure gets somewhat affected by Li^{3+} ion irradiation.The presence of many new peaks with the increase of fluence suggests the formation of alkenes and alkynes which might be responsible for changing the dielectric constant and tan δ values.

The ion irradiation of PP films leads to chain scission and cross linking and as a result there are changes in the dielectric properties. The value of the dielectric constant and loss factor increases with increase in fluence. The loss factor shows a moderate increase up to 10 kHz frequency at all temperatures suggesting that PP film capacitor may be useful below 10 kHz frequency. The data obtained from the thermograms of PP, suggest that the decomposition nature of the polymer changed due to the Li^{3+} ion irradiation. This denotes a degradation of the polymer matrix under Li^{3+} ion irradiation making the irradiated polymer to decompose earlier than the pristine sample.

4.2   Polyethylene Terephthalate (PET)

As discussed in chapter 3 (article 3.2.1) we know that, PET is a thermoplastic polyester with a high melting point (~265°C) and very good mechanical strength (at least up to 175°C) due to the presence of the aromatic ring in the polymeric structure. It is resistant to heat and moisture and virtually immune to many chemicals and used extensively in fiber and sheet form. It has good gas barrier properties and good chemical resistance except to alkalis (which hydrolyse it). It is used in the manufacture of containers, such as milk bottles and laundry detergent jugs. Transparent sheets and castings can be formed from this polymer. 'PET' films are used for capacitors, graphics, film base and recording tapes etc. besides in wide applications for nuclear and space technologies. It is used in garment manufacture, magnetic recording tapes, aluminized sheets.

Literature surveys reveal that the effects of ion beam irradiation on polyethylene terephthalate (PET) have been studied extensively.

Ciesla and Starosta [12] studied the effect of high energy heavy ions on PET films at high fluence using, DSC, FTIR and XRD studies. DSC revealed the amorphization of PET films after heavy ion irradiation. Differences in melting and crystallization processes between pristine and irradiated samples were observed on primary heating but also on cooling and repeated heating. The decrease in crystallinity was confirmed by wide and small angle XRD and volume crystallinity measurements. The amorphization is due to cross-linking and degradation processes. The changes in irradiated PET revealed by IR spectroscopy can also be attributed to an increase of the content of amophization phase.

Steckenreiter et al [13] showed the chemical modification of PET induced by swift heavy ions. The irradiations with Kr (8.6 MeV/u) and with Mo (5.6 MeV/u) ions were performed under vacuum and in oxygen atmosphere, respectively. The overall degradation of polymer was investigated as a function of fluence. A significant loss of crystallinity is related to scission processes of the main chains at the ethylene glycol residue. The benzene ring structure shows only small changes under irradiation and do not seem to participate in the degradation process significantly. While various degradation processes known from photochemical degradation takes place, the creation of alkynes near the track core is found to be a unique process induced by heavy ions. The presence of oxygen during irradiation enhances the overall degradation of PET leads to enhanced formation of alkynes and CO_2.

Biswas et al [14] studied the effect of swift heavy ion irradiation on the radiochemistry and melting characteristics of PET by using FTIR and DSC measurements. After irradiation with a 180 MeV Ag^{14+} ion beam, DSC measurements of PET films exhibited significant change in their melting behaviour. The gradual increase in the melting enthalpy of irradiated PET with the ion fluence is observed, which reaches a maximum when track overlapping sets in, and decreases exponentially thereafter. FTIR measurements of irradiated PET at different ion fluences have also shown partly different trend of amophisation. X-ray diffractions results of irradiated PET revealed a shift and reduction of the main peak alongwith the appearance of a new small peak.

Tripathy et al [15] studied the proton induced modification in polyethylene terephthalate. A systematic investigation of 62MeV proton irradiated PET has been

carried out using FTIR spectroscopy, thermogravimetric analysis, differential scanning calorimetry and X-ray diffraction spectrometry. The experiments revealed a restoration of the crystalline matrix and simultaneous decrease in thermal stability in the irradiated polymer as a function of dose, indicating that PET underwent both degradation and cross-linking by proton irradiation.

Bridwell et al [16] studied the electrical conductivity of PET by implanting He, B, C, N and Ar at an energy of 50 KeV. Surface resistivity v/s dose in the range $10^{16} - 10^{17}$ ions/cm^2 indicates a plateau effect that is dependent on the incident ion and the target polymer. They observed that aliphatic or partially aliphatic polymer (PET) will reach lower resistivity than the fully aromatic polymer.

Ueno et al [17] studied the effects of high energy ion beam irradiation on PET films using 3MeV O, Ni, Pt, and Au ions by surface resistivity measurement and RBS. The surface resistivity decreases with increasing irradiation dose. From RBS analysis, they reported the case of bond destruction of PET molecular structure under irradiation.

But detailed studies of dielectric properties at different temperatures and frequencies are not much reported. Although the published literature contains numerous studies of its physical properties, most dielectric investigations have covered a limited temperature-frequency range or have concentrated on particular factors affecting the dielectric response. In this study, polyethylene terephthalate (PET) films were irradiated with 50MeV Li^{+3} ions using 15UD pelletron at the Nuclear Science Center,

New Delhi, India. The radiation induced changes in electrical property, microhardness, thermal stability and structural changes are investigated using variable frequency LCR meter, Vicker's microhardness indenter, TGA and FTIR spectroscopy respectively [18-20].

4.2.1   Structural Analysis

The FTIR spectra of pristine and irradiated samples are shown in **Figure 4.12**. The absorption bands as obtained from the spectrum of pristine PET are identified as (A) 725 cm^{-1} : ring of deformation of phenyl ring, bending vibration of CH_2 group (B) 862cm^{-1} : C-H deformation of phenyl ring, vibration band of para substituted benzene ring (C) 1013cm^{-1} : C-O-C stretching of ester (D) 1347cm^{-1} : C-C stretching of phenyl ring vibration band of para substituted benzene ring (E) 1700 cm^{-1} : C=O stretching vibration (F) 2972 cm^{-1} : C-H stretching of CH_2 group. Most of the peak positions were found to be unshifted. Only the absorbance or transmittance value of particular functional groups changed. This might be attributed to breakage of chemical bonds and the formation / emission of low molecule gases and radicals due to ion beam irradiation. However, the large number of bands observed between 3000 and 3700cm^{-1} are difficult to explain. Such bands are generally observed in amides or alcohols. The absence of –OH- or –NH- bands in the polymer structure made it difficult to explain these bands. However, we believe that the atmospheric oxygen and water interaction with the surface of the polymer probably gave rise to these bands which get somewhat modified on irradiation.
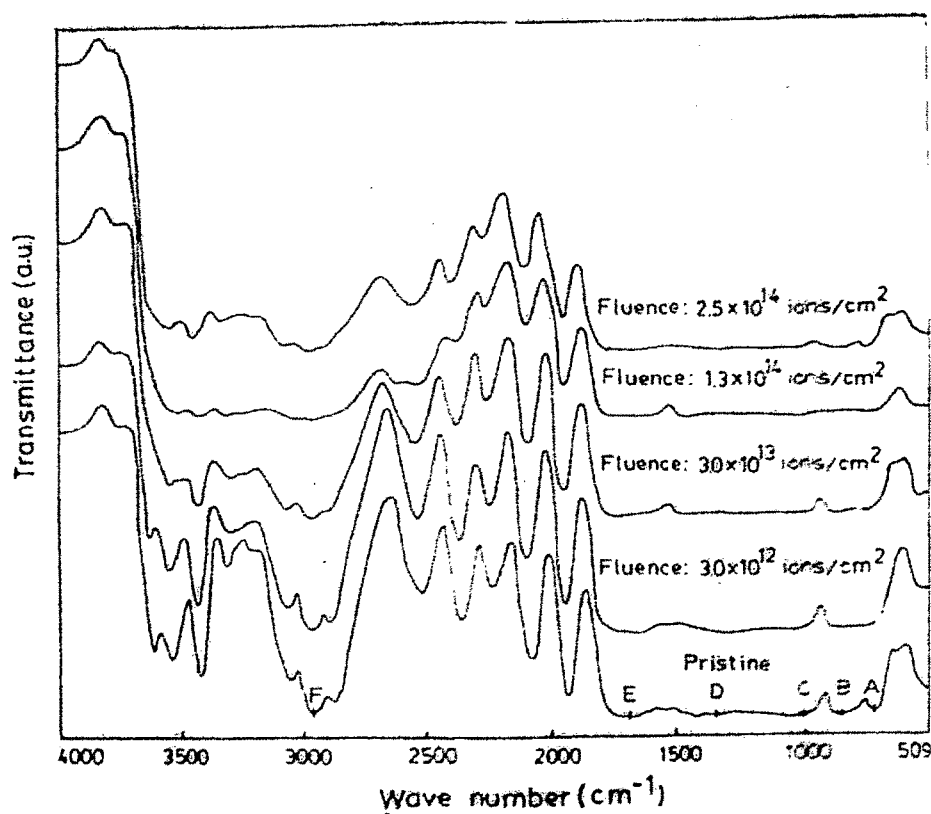
Figure 4.12   FTIR spectra of Pristine and Irradiated PET samples

4.2.2   Electrical Properties of Polyethylene Terephthalate.

The electrical properties of pristine and irradiated PET samples were measured using an LCR meter. The frequency was varied from 0.05 to 100KHz, while the temperature was varied from ambient to 150°C respectively. Resistivity and conductivity were calculated using the formula given by equations (2.4) and (2.5) in article 2.3.1 (c) of chapter 2. The dielectric constant was calculated using the formula given by equation (2.9) in article 2.3.1 (d) of chapter 2. The findings with their respective explanations are as follows.

4.2.2 (a) log Resistivity v/s log Frequency

Figure 4.13 shows the dependence of the resistivity of PET film on frequency at different temperatures keeping fluence constant. It is seen that resistivity decreases rapidly as frequency increases. It is also observed that resistivity decreases as temperature increases.

Figure 4.14 shows the dependence of resistivity of polymer (PET) films on frequency at ambient temperature for pristine and irradiated samples. It is seen that resistivity decreases rapidly as frequency increases. It is also observed that resistivity decreases as fluence increases. An AC field of sufficiently high frequency applied to a metal-polymer-metal structure may cause a net polarization, which is out of phase with the field. This results in AC conductivity, it appears at frequency greater than that at which traps are filled or emptied [6,7].
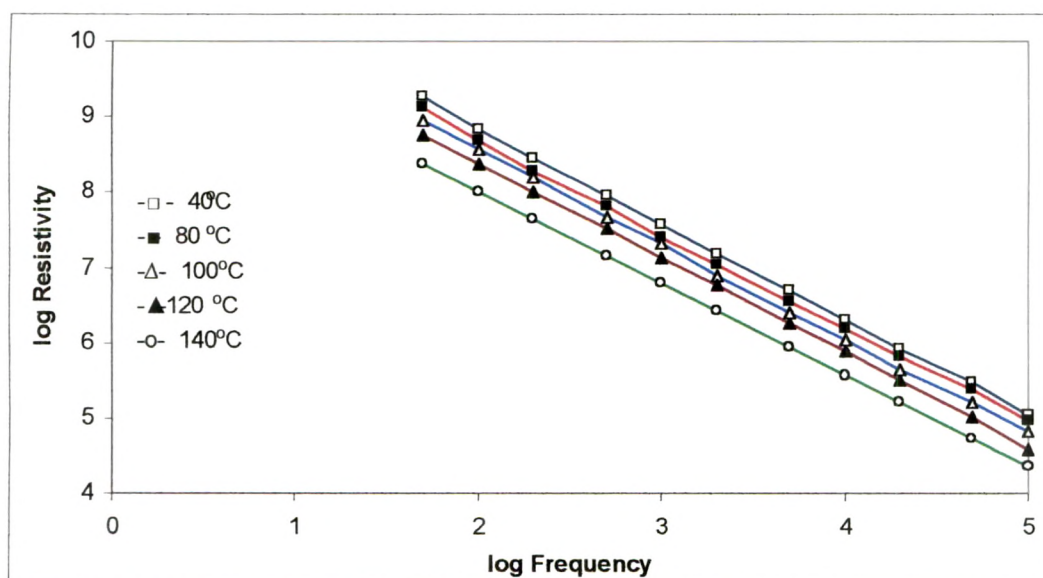

Figure 4.13 Plot of log Resistivity v/s log Frequency(f in Hz) at different temperatures (°C), keeping fluence (1.3 x 10^{14} ions/cm^2) constant
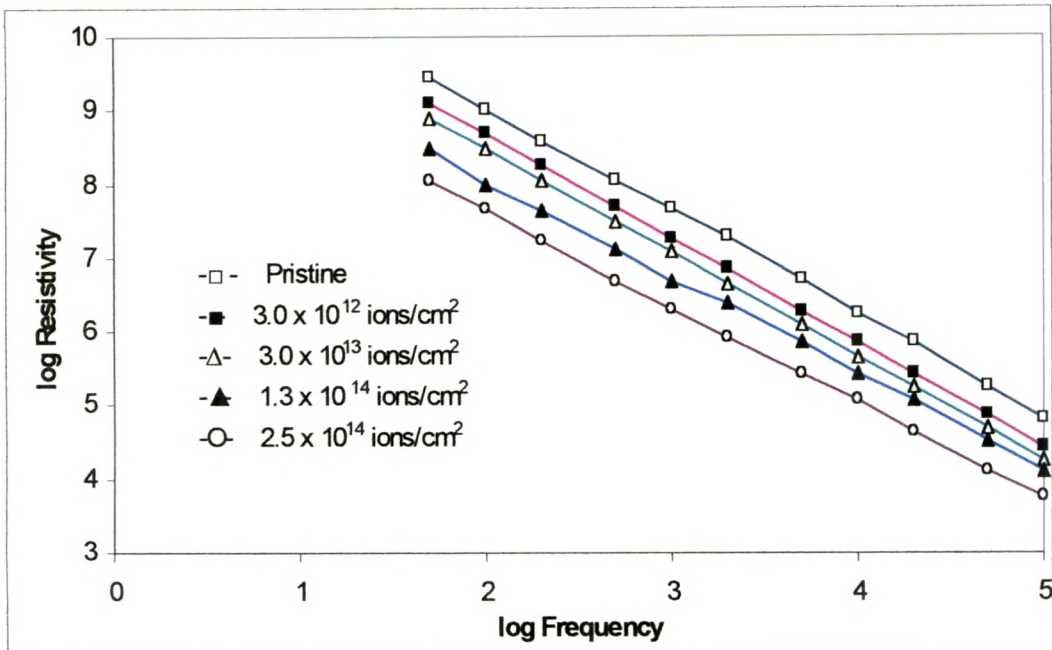
Figure 4.14 Plot of log Resistivity v/s log Frequency (f in Hz) at different fluence keeping temperature constant.

4.2.2(b) Conductivity v/s log Frequency

Figure 4.15 shows the dependence of conductivity (inverse of resistivity) of PET films on log frequency (f in Hz) at ambient temperature for pristine and irradiated samples. A sharp increase in conductivity has been observed at 20kHz. It is also observed that conductivity increases as fluence increases. The increased conductivity due to irradiation may be attributed to scissioning of polymer chains and as a result increase of free radicals, unsaturation etc. When an ac field of sufficiently high frequency is applied to a metal-polymer-metal structure, it may cause a net polarization which is out of phase with the field. This results in ac conductivity. It appears at a frequency greater than that at which traps are filled or emptied.
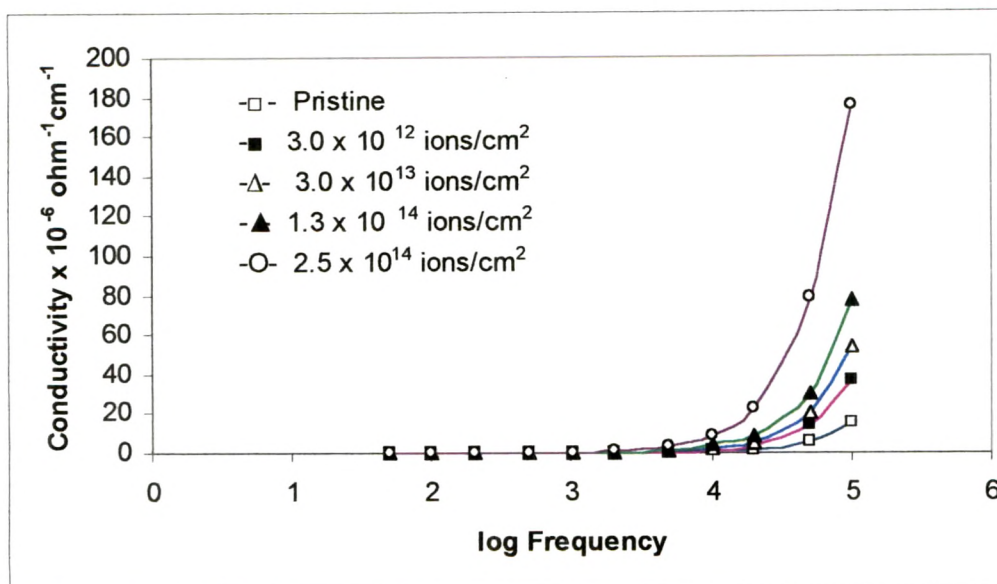
Figure 4.15 Plot of Conductivity v/s log Frequency (f in Hz) for Pristine and Irradiated PET samples at ambient temperature.

4.2.2 (c) tan δ v/s Temperature

The study of the dielectric response of unirradiated and irradiated films of a material provides information about the orientation and translational adjustment of mobile charges present in the dielectric medium in response to an applied electric field. Hence this study.

Figure 4.16 shows the behaviour of dielectric loss with temperature at 10 kHz for pristine and irradiated samples. The relaxation peak is observed at 60°C. When polymer is heated the movement of the large segments of the main chain sets in becoming a maximum at Tg at which the loss tangent maximum occurs corresponding to the relaxation peak of the thermally stimulated discharge[10]. It is observed that dielectric loss increases with the increase of temperature. The value of tan δ is also found to

increase with increasing fluence. The dielectric loss is due to the perturbation of phonon system by an electric field, the energy transferred to the phonon is dissipated in the form of heat. The growth in tan δ and thus decrease in resistivity (and increase in conductivity) is brought about by an increase both in the conduction of residual current and the conduction of the absorption current [7].

Figure 4.17 shows the behavior of dielectric loss with temperature in the temperature range $40 - 150^\circ C$ and at frequencies of 1 kHz, 10 kHz and 100 kHz keeping fluence constant. It is observed that dielectric loss increases with the increase of temperature at all frequencies. The relaxation peak corresponding to T_g may also be understood by the free volume theory put forward by Fox and Flory [21]. According to this theory, the molecular mobility (and consequently the relaxation time) near T_g depends mainly on the free volume. In the glassy state below T_g the free volume will be frozen in and will remain at a constant value, the hole size and distribution of free volume remains fixed. As the temperature increases the glassy state will expand due to the normal expansion of all the molecules, which results from the changing vibrational amplitudes of bond distances [22]. As T_g is reached, in addition to the normal expansion process, there will be an expansion of the free volume itself, which results in a larger expansion of the rubber-like polymer. This yields sufficient room for the rotation or translation motion of the molecules to occur. Due to this increase in chain segment mobility, there will be a very large increase in the dissipation factor at T_g. This effect can be clearly seen in the figure 4.16 and 4.17 respectively.
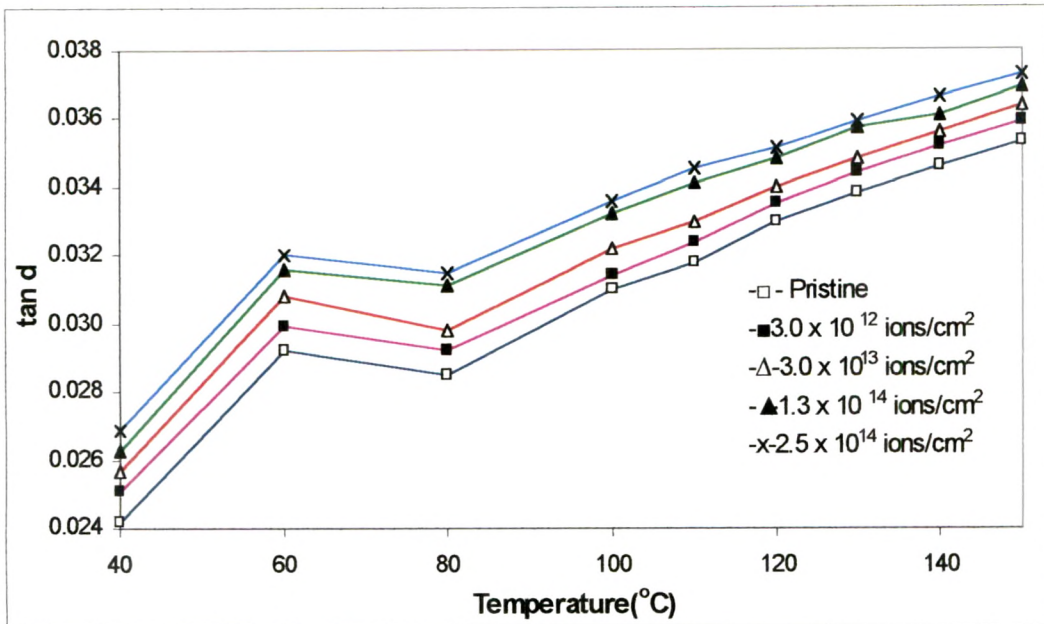
Figure 4.16 Plot of Dissipation factor (tan δ) v/s Temperature (^{o}C) for pristine and irradiated PET samples at 10kHz frequency.
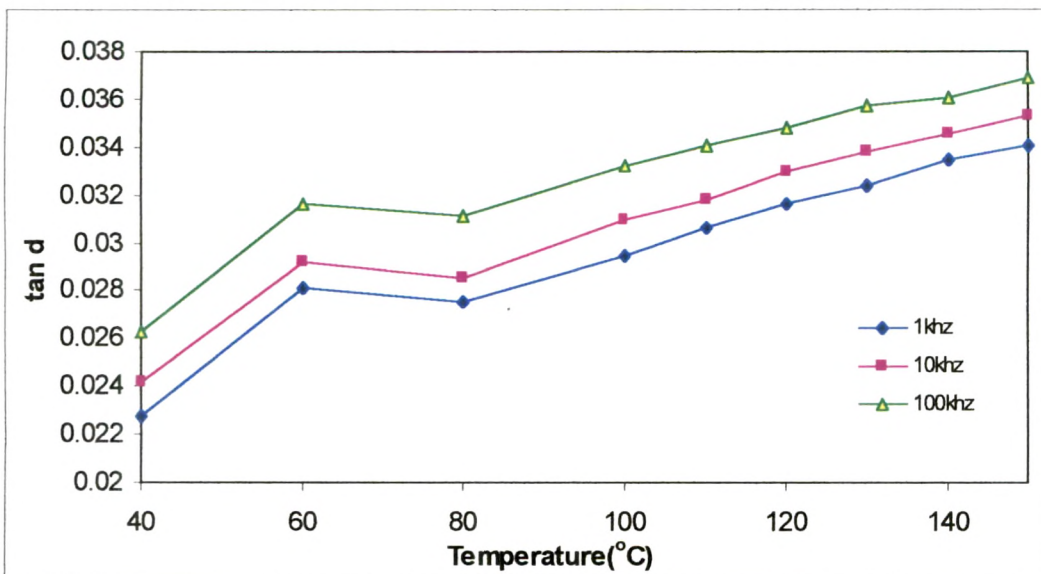

Figure 4.17 Plot of Dissipation factor (tan δ) v/s Temperature (^{o}C) at different Frequency keeping fluence (1.3 x 10^{14} ions/cm^{2}) constant.

4.2.2 (d) tanδ v/s log Frequency

Figure 4.18 shows the behavior of tan δ measured as a function of frequency at different temperatures keeping fluence constant (1.3×10^{14} ions/cm^2). It is observed that with the increase in frequency, dielectric loss shows moderate increase up to 10kHz at all temperatures, suggesting that PET films can be used as a dielectric in capacitors being used below 10kHz frequency.

Figure 4.19 shows the behavior of tan δ measured as a function of log frequency at different fluences at ambient temperature. It is observed that the loss factor increases moderately as frequency increases. It is also observed that the loss factor increases as fluence increases. The growth in tan δ and thus decrease in resistivity is brought about by an increase in the conduction of residual current and the absorption current [6].
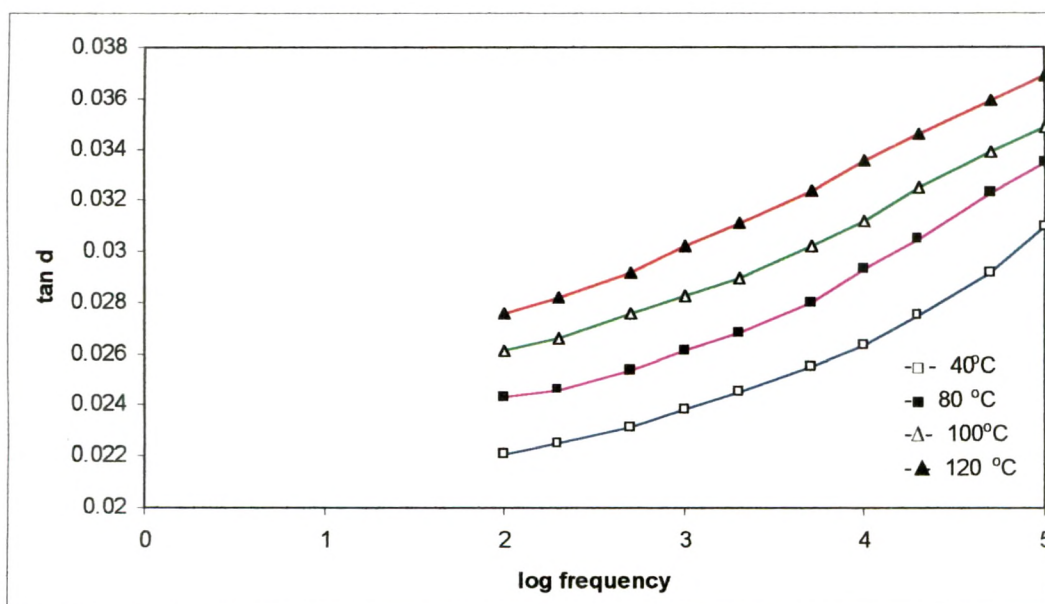
Figure 4.18 Plot of Dissipation factor (tan δ) v/s log Frequency at different temperature (°C), keeping fluence (1.3×10^{14} ions/cm^2) constant.
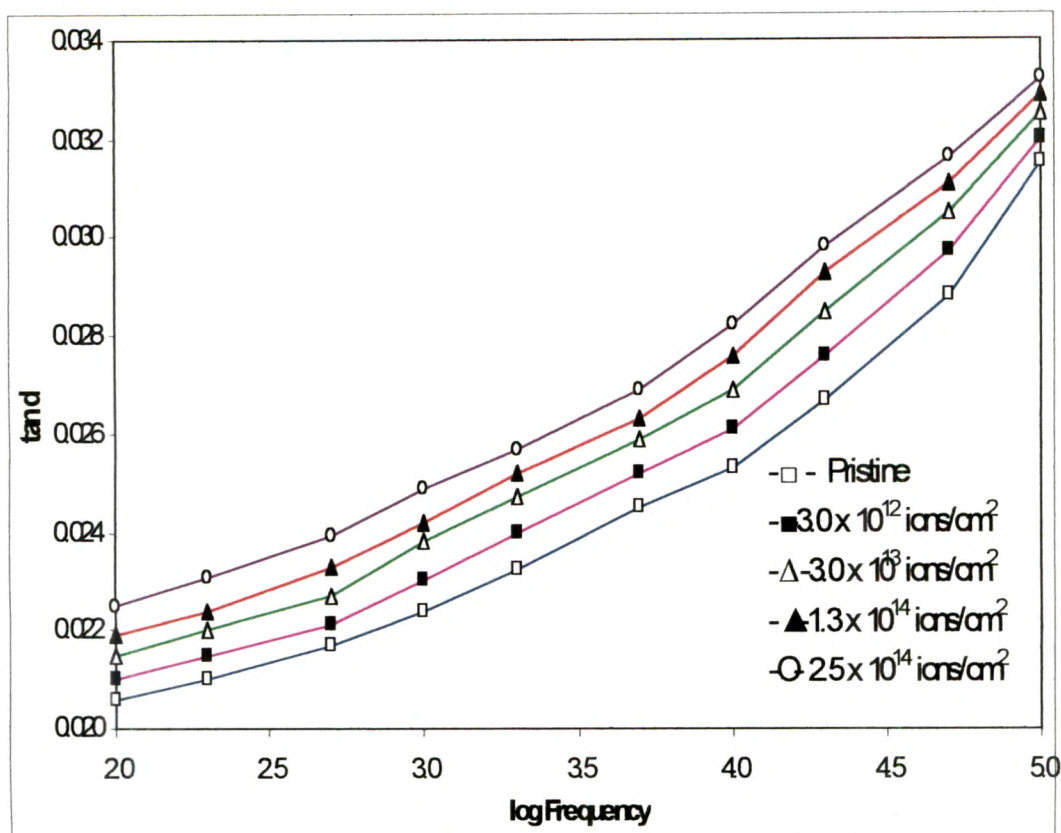
Figure 4.19 Plot of Dissipation factor (tan δ) v/s log Frequency at different fluence at ambient temperature

4.2.2 (e)   **Dielectric Constant v/s log Frequency**

Figure 4.20 shows the behavior of dielectric constant as a function of frequency at different fluences. It is observed that dielectric constant remains constant in the frequency range 0.05-100kHz. At these frequencies, the mobility of the free charge carriers is constant and thus dielectric constant is constant [11]. It is also observed that dielectric constant increases as fluence increases. The increase in dielectric constant may be attributed to chain scission and as a result increase of free radicals etc.
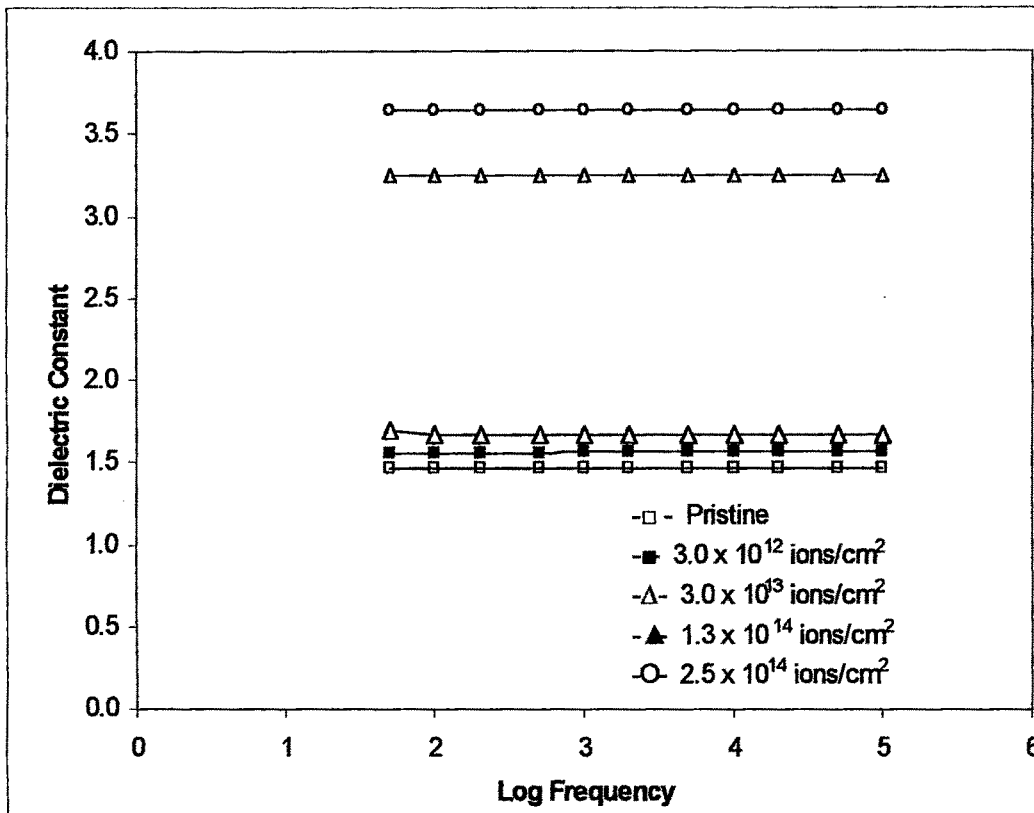
Figure 4.20 Plot of Dielectric Constant v/s log Frequency (f in Hz) at different fluences.

4.2.2 (f)   Dielectric Constant v/s Temperature

Figure 4.21 shows the dielectric constant as a function of temperature at a frequency of

10KHz. The dielectric constant is almost constant with change of temperature. The

negligible change (about 6%) in dielectric constant with temperature could be due to

the effect of conductance corresponding to absorption current. It is also observed that

dielectric constant increases as fluence increases at a certain temperature. This increase

in dielectric constant may be attributed to the increase of free radicals etc.
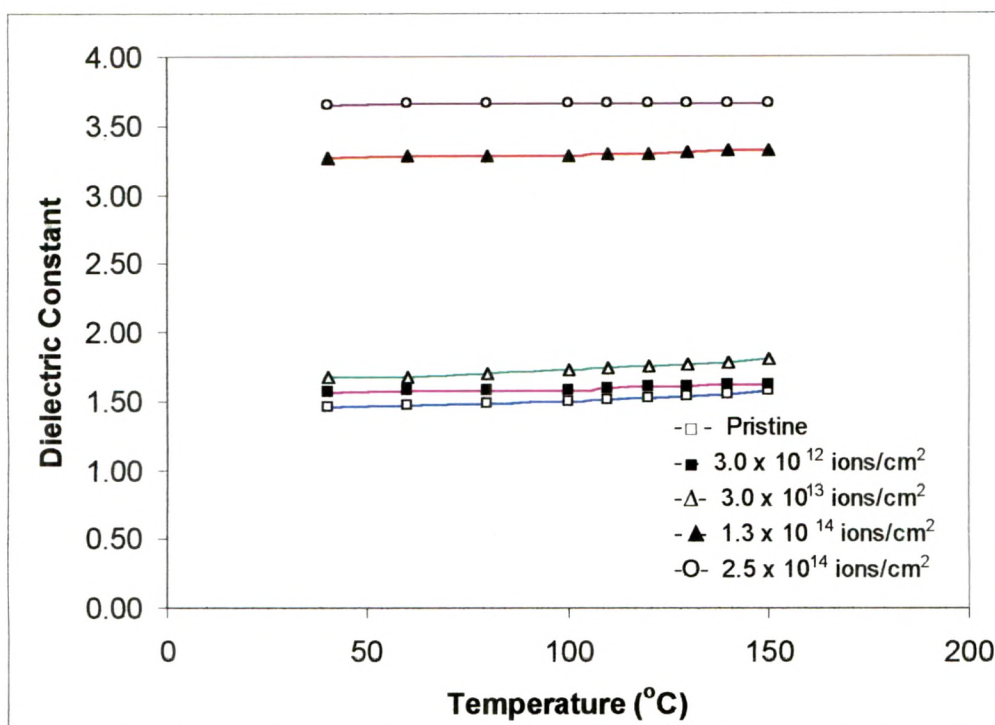
Figure 4.21 Plot of Dielectric Constant v/s Temperature (°C) at different fluences.

4.2.3   Thermal Analysis of Polyethylene Terephthalate (Thermogravimetric analysis)

The decomposition behaviour of the pristine and the irradiated (at the fluence of 1.3×10^{14} ions/cm^2) polymers were studied by this technique. The thermograms are as shown in the **Figure 4.22** and the temperature along with the respective weight loss (%) for different zones is given in **Table 4.2**. It is quite evident from the thermograms that there is a decrease in thermal stability due to Li^{3+} ion irradiation. The pristine sample remains stable upto 220°C, where no weight loss of the sample takes place. This stable zone is followed by a slow rate of decomposition from 220 to 360°C. In this slow decomposition zone, there is a weight loss of about 12%. A faster rate of decomposition

starts after that till the sample is completely decomposed at 560°C. A weight loss of about 88% has been recorded in this zone. The irradiated polymer remains stable up to a temperature of about 120°C. A slower rate of decomposition takes place from 120-280°C, where the sample losses its weight by about 16 % of its original weight. This is followed by a fast decomposition zone from 280°C – 480°C with a weight loss of about 84%. The irradiated sample gets completely decomposed at 480°C. This denotes a degradation of the polymer matrix under Li^{3+} ion irradiation making it decompose earlier than the pristine sample.
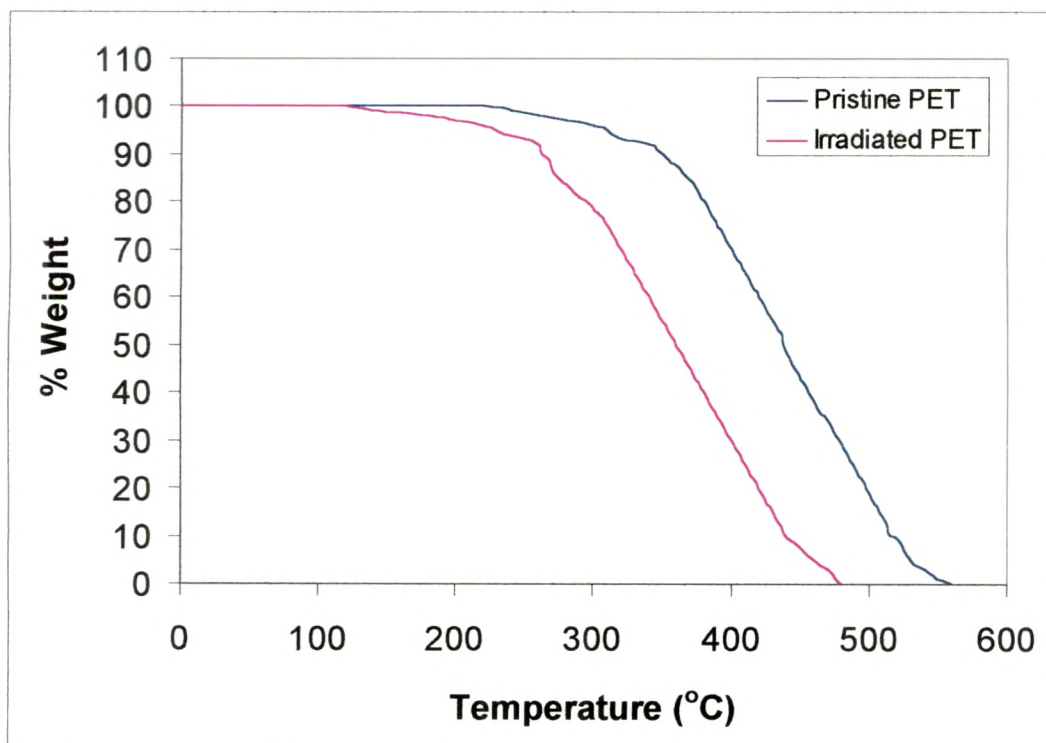

Figure 4.22   TGA thermograms of Pristine and Irradiated (fluence of 1.3 x 10^{14} ions/cm^2) PET films.

Table 4.2   **Data derived from TGA thermogram of pristine and irradiated PET**

denoting their thermal decomposition behaviour.

Sample Weight (mg)	Zone	Temperature Range	Weight loss (%) in zone	Total Weight loss (%)	Remark
Pristine	I	0°C to 220°C	0	0	Stable Zone
	II	220°C to 360°C	12	12	Slow Decomposition
	III	360°C to 560°C	88	100	Fast Decomposition
Irradiated	I	0°C to 120°C	0	0	Stable Zone
	II	120°C to 280°C	16	16	Slow Decomposition
	III	280°C to 480°C	84	100	Fast Decomposition

4.2.4   Mechanical Property of Polyethylene Terephthalate (Microhardness).

We have studied the mechanical property (microhardness) by means of Vicker's microhardness indenter. The Vicker's hardness was calculated using equation 2.15 as discussed in chapter 2.

Figure 4.23 shows the plots of the Vicker's microhardness (H_v) v/s applied load P at different fluences. It is observed that the hardness increases with load up to 500mN and then saturates beyond the load by 500mN. The increase in H_v with load can be explained on the basis of the strain-hardening phenomenon. On applying the load, the polymer is subjected to some strain hardening. Beyond a certain load the polymer exhausts its strain hardening capacity and the hardness tends to become constant.

The rate of strain hardening is greater at low loads and decreases at higher load. As can be seen, hardness becomes independent of load for more than 500mN. The value obtained from the saturation region, therefore represents the true hardness of the bulk material, since at high loads the indenter penetration depth is also high and surface effects become insignificant. It is also observed that the hardness increases as fluence increases. This may be attributed to the cross-linking phenomenon [23].

From **Figure 4.24** it is observed that hardness increases as ion fluence increases. The increase in the crystallisation (i.e. cross-linking phenomenon) may have resulted in the increase in microhardness.
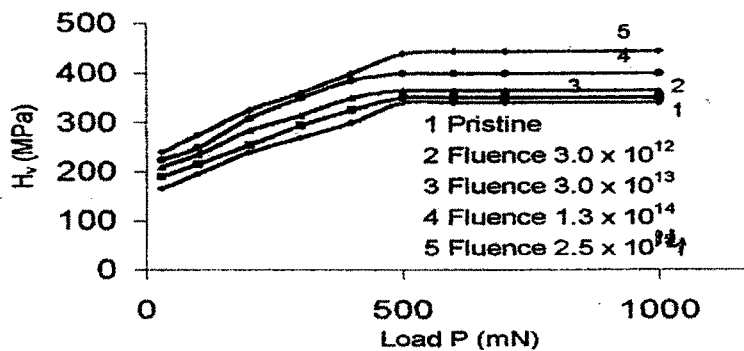

**Figure 4.23**   **Plot of Microhardness v/s Applied load for pristine and irradiated PET films.**
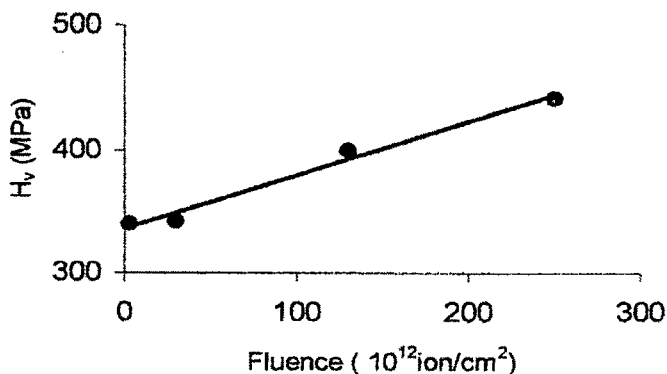
Figure 4.24   **Plot of Hardness v/s Fluence of PET samples.**

4.2.5 Conclusion

FTIR spectra of this polymer before and after irradiation indicates that various bands related to C-H stretching of CH_2 group at 2972 cm^{-1}, C=O stretching vibration at 1700 cm^{-1}, C-O-C stretching of ester at 1013 cm^{-1} and bending vibration of CH_2 group at 725 cm^{-1} are modified. It is also inferred from FTIR spectra that there is no significant change in overall structure of polymer but a minor change in intensities have been observed up to the fluence of 3.0×10^{13} ions/cm^2. This might be due to the breakage of a few bonds in the structure. It may be concluded that PET is resistant to radiation atleast up to the fluence of 3.0×10^{13} ions/cm^2. The ion irradiation of PET films leads to chain scission and as a result there are changes in the dielectric properties. The value of the dielectric constant and loss factor increases with increase in irradiation fluence. The loss factor shows a moderate increase up to 10kHz frequency at all temperatures suggesting that PET film capacitors may be useful below 10kHz frequency. The irradiated sample starts decomposing at a comparatively lower temperature compared to the pristine sample. This denotes a degradation of the polymer matrix under Li^{3+} ion irradiation making it decompose earlier than the pristine sample. It is observed that the hardness increases with load up to 500mN and then saturates beyond the load of 500mN. The true bulk hardness of the film is obtained at loads greater than 500mN. The increase in H_v with load can be explained on the basis of the strain-hardening phenomenon. It is also observed that the hardness increases as fluence increases. This may be attributed to the cross-linking phenomenon.

4.3 KAPTON (POLYIMIDE)

As discussed in chapter 3 (article 3.2) we know that polyimide is a yellow coloured, transparent, soft, thermoplastic polymer. Kapton is one of the most important electrically insulating polymers as it has good ultimate tensile strength (UTS) and its working temperature ranges from liquid helium's temperature to $200^{\circ}C$ in a continuous use. It is noteworthy that now a days, polymers are included as nuclear materials as well as insulating materials in nuclear fusion reactors. Glass fiber filled (GFF) polyimide is a very promising material for super conducting magnet coil insulation in radiation environments. Further in a nuclear reactor containment building, there are a large number of electrical components and scales made of polymeric materials which may get radiation doses as high as 5×10^8 Rad. It is desirable that they should remain unaffected even after exposure to such high doses.

The effects of KeV and MeV ion beam irradiation on Kapton (PI) have been studied extensively. The reported works are as follows.

Shrinet et al [24] studied the blisters formation on Kapton surface using 250KeV H^+ ion at the dose of 7×10^{15} ions / cm^2. The observed features are explained on the basis of the aliphatic C-H bond breakage theory due to ion bombardment.

Xu et al [25] studied ion beam induced chemical and structural modifications in PI films. It is found that chemical structure in PI is subjected to a severe alteration within the dose range from 10^{14} to 10^{15} B^+/cm^2. The radical structure modification is completed only as irradiation reaches 10^{16} B^+/cm^2, at which point one may find that

there exists a resemblance in profile shape between the IR spectrum of the high dose irradiated PI film.

Fink et al [26] investigated the IR transmission spectra for keV to MeV light and heavy ion irradiated PETP, PMMA, PC and PI films. Changes in most preexisting transmission dips have been observed as a function of the irradiation dose but no additional new IR absorption structures have been recorded after irradiation.

The change in composition and structure of PI films due to irradiation induced carbonization was studied by surface characterization techniques and electric resistance measurement by Terai and Kobayashi [27]. This study was done by irradiating PI films using 4MeV Ni^{3+} ions in the fluence range 3.5 x 10^{12} to 1.0 x 10^{16} ions/cm^2. They reported that the electric resistance of the film became very high in the high fluence region of 10^{15} ions/cm^2, which comes from the dispersion of the carbonized areas in the insulating matrix.

Virk et al [28] studied the effects of 70 MeV carbon ion on the physical and chemical response of PI by using UV-visible, FTIR and XRD techniques in the fluence range 9.3 x 10^{11} to 9 x 10^{13} ions/cm^2. UV- visible spectroscopic analysis of irradiated kapton reveals a change in optical density and creation of defects, which may be due to both degradation and cross linking of polymer chains simultaneously. FTIR analysis revealed that ring or ladder-structured polymers are chemically highly resistant to electronic energy loss. PI has partial crystallinity as seen in XRD patterns.

A systematic investigation of 62 MeV proton irradiated polyamide has been carried out using some spectroscopic and thermal techniques by Mishra et al [29]. It was concluded by them that there was no prominent variation in the absorbance bands of PI by proton
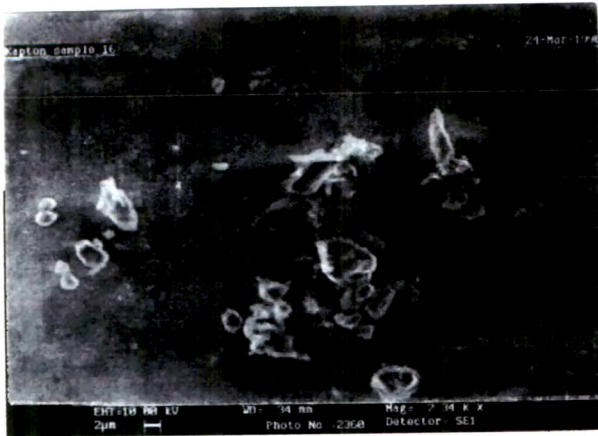
Figure 4.26 (a)   SEM picture of irradiated kapton film at the fluence of 5.2 x 10^{13} ions/cm^2.

Figure 4.26(b) SEM pictureof irradiated kapton film at the fluence of 1.0 x 10^{14} ions/cm^2.


Figure 4.26(c) SEM picture of irradiated kapton film at the fluence of 1.0x10^{14} ions/cm^2.

4.3.2 Microhardness.

We have studied the mechanical property (microhardness) by means of Vickers' microhardness indenter. The Vickers' hardness was calculated using equation 2.15 (article 2.3.5) as discussed in chapter 2.

Figure 4.27 shows the variation of the Vickers' Microhardness (H_v) with an applied load (P) for pristine and irradiated films. It is evident from figure 4.27 that the H_v value increases with load up to 300mN and then saturates beyond the load of 400mN. The increase in H_v with load can be explained on the basis of the strain hardening phenomenon. On applying the load, the polymer is subjected to some strain hardening. Finally, when H_v value tends to become constant, the polymer is completely strain hardened. Beyond certain load the polymer exhausts its strain hardening capacity and the hardness tends to become constant. The rate of strain hardening is greater at low loads and decreases at higher loads [23,35]. As can be seen, the hardness becomes independent of load for more than 400mN. The value obtained from the saturation region, therefore represents the true hardness of the bulk materials, since at high loads the indenter penetration depth is also high and surface effects become insignificant. It is also observed that the hardness increases as fluence increases. The increase in hardness, as a result of increase in fluence can be assigned to the cross-linking phenomenon affected by electronic stopping [23].
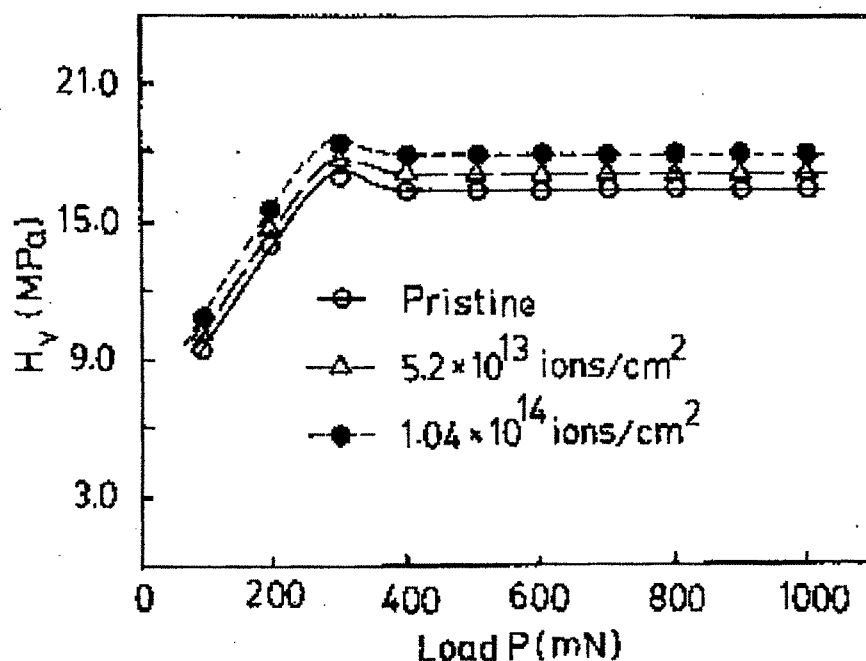
Figure 4.27 Plot of Microhardness v/s applied load for pristine and irradiated kapton films.

4.3.3 Structural Analysis

To investigate the reason for the formation of blisters on kapton surface, FTIR spectra were carried out for the irradiated and pristine films in the wave number range 500 to 4000cm^{-1}. The FTIR spectra of these films in the transmission mode are shown in **Figure 4.28**. It is observed that there is no change in overall structure of the polymer, but minor change in intensities have been observed, which implied that inter-chain separation is not affected much by Li^{3+} ion irradiation [28]. Most of the peak positions were found to be unshifted. Only the absorbance or transmittance value of the

functional groups indicated below changed. They might be due to a decrease in concentration of the pre-existing bonds or groups.

The absorption bands, as obtained from the pristine spectrum, are identified as (A) 1723 cm^{-1}; C=O stretching vibration, (B) 3074 cm^{-1}; aromatic C-H stretching, (C) 3486 cm^{-1}, N-H bending vibration, (D) 3630 cm^{-1}; OH stretching vibration. The absorbtion bands at 1723, 3074, 3486 and 3630 cm^{-1} are selected for this analysis, since they have a relatively large absorbance. It is found that the absorption bond characteristics of all the above functional group exist even after the fluence of 1.04 x 10^{14} ions / cm^2. The minor decrease in the intensity of these functional groups (i.e. 1723, 3074, 3486 and 3630 cm^{-1}) is attributed to the emission of adsorbed gases just below the surface. It is inferred that the reduction in specific height is due to the deterioration of these groups in the form of H_2, CO or CO_2 gas. The release of H_2/CO/CO_2 gas results in the blister formation on the surface of thermally stable kapton film. The minor changes in the peaks of the irradiated sample may be due to the breakage of one or two bonds in the ladder structure, but this will not change the overall structure of the polymer [24,25,28]. From these observations it may be concluded that kapton is highly resistant to radiation degradation.
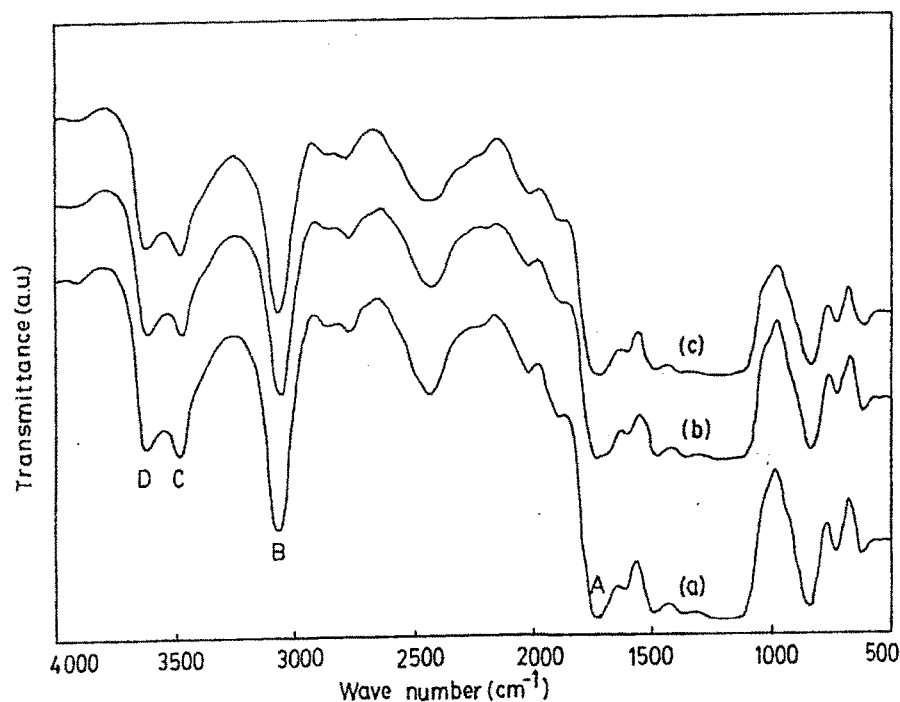
Figure 4.28 FTIR Spectra of Pristine and irradiated Kapton samples.

4.3.4   Conclusion

The blisters formation on the surface of the kapton are attributed to breakage of chemical bonds and the formation of low molecule gases. These gases are accumulated inside the polymer at a depth where maximum radiation damage takes place. When the pressure of accumulated gas crosses the mechanical strength of the kapton film, it deforms and results as blisters. The emission of low molecular gases (i.e. CO and H_2) is also confirmed by the FTIR analysis of the irradiated kapton films. The irradiation has been found to increase the Vickers' hardness of the kapton film significantly .The true bulk hardness of the film was obtained at loads greater than 400 mN.

4.4   Blended Polymer (PVC and PET).

The most exciting development in recent years has been the introduction of several new types of polymeric blends. They are generally made by blending thermoplastic with a suitable polymer. Thermoset material cannot be reprocessed and cannot be used again. In contrast polymeric blend materials can be repeatedly softened by heating to the moulding temperature and scrap material / parts can be efficiently reprocessed. The significant advantage of polymer blends is that the properties of the finished product can be tailor made to the requirements of the application, which cannot be achieved either alone by one polymer. The polymeric blends are accepted as engineering plastic materials due to their better mechanical and electrical properties. Polymers find increasing usage in different technological applications, e.g. in micro-electronics, optics and medicine.

In India various types of domestic switches are being manufactured and these are made from either urea/phenol formaldehyde resin or polycarbonates. The former materials are cheaper, light in colour, have better resistance to electrical tracking but have inferior heat resistance, are brittle and have higher water absorption where as polycarbonates are quite expensive and required special care during processing. Moreover, polycarbonates have limited resistance to chemical (like toluene) and UV light. These switches are subjected to mechanical, electrical and thermal stress during their operation.

No work has been reported so far on the change in properties of blended polymeric films due to ion irradiation. With growing interest in the modification of various polymers through the technique of ion irradiation, both the properties and the

corresponding microstructures of the high fluence irradiated polymeric films have been investigated. The deposited energies effectively modify the chemical structure of the polymers resulting in changes in the electrical conductivity, hardness, thermal properties etc.

Blend of PVC and PET was made to obtain desirable properties better compared to the individual polymer properties. The objective of the present work is to develop polymeric blend for industrial application needs such as: sensors, rechargeable batteries etc, domestic switch gear and to study the effects of high energy ions on its thermal and structural behaviors.

As part of the work for this thesis, a study of the effect of 50 MeV Li $^{3+}$ ion irradiation on structural, electrical, thermal, and application of blended polymer (PVC + PET) as a sensor has been undertaken. The change in structural property was studied using FTIR spectroscopy, electrical property using an LCR meter, thermal stability by TGA was studied for both pristine and irradiated films. Polymer blend of Poly vinyl chloride (PVC) and Polyethylene terephthalate (PET) i.e. PVC + PET have been prepared as mentioned in chapter 3 (article 3.3.1). Blend of PVC + PET was made in 50:50 proportion.

4.4.1   Structural Analysis.

FTIR spectra of pristine and irradiated samples are shown in the above **Figure 4.29.** The absorption bands as obtained from the spectrum of pristine are identified as (A) 600-800cm^{-1}; C-Cl stretching vibration, ring deformation of phenyl ring, (B) 1015 cm^{-1};   C-O-C stretching of ester, (C) 1520 cm^{-1}; C-C stretching of phenyl

group, (D) 1730 cm^{-1}; C=O stretching vibration, (E) 2800-3000cm^{-1}; C-H stretching of CH$_2$ group, (F) 3258 cm^{-1}; C-H stretching vibrations of the alkyne group, (G) 3000-3600 cm^{-1}; OH stretching vibration [13,14] .

It is found that the absorption bands characteristic of all previously mentioned functional groups declines, conforming their destruction by irradiation and they vanish gradually as irradiation proceeds. This might be attributed to breakage of chemical bonds and the formation/emission of low molecule gases and radicals.
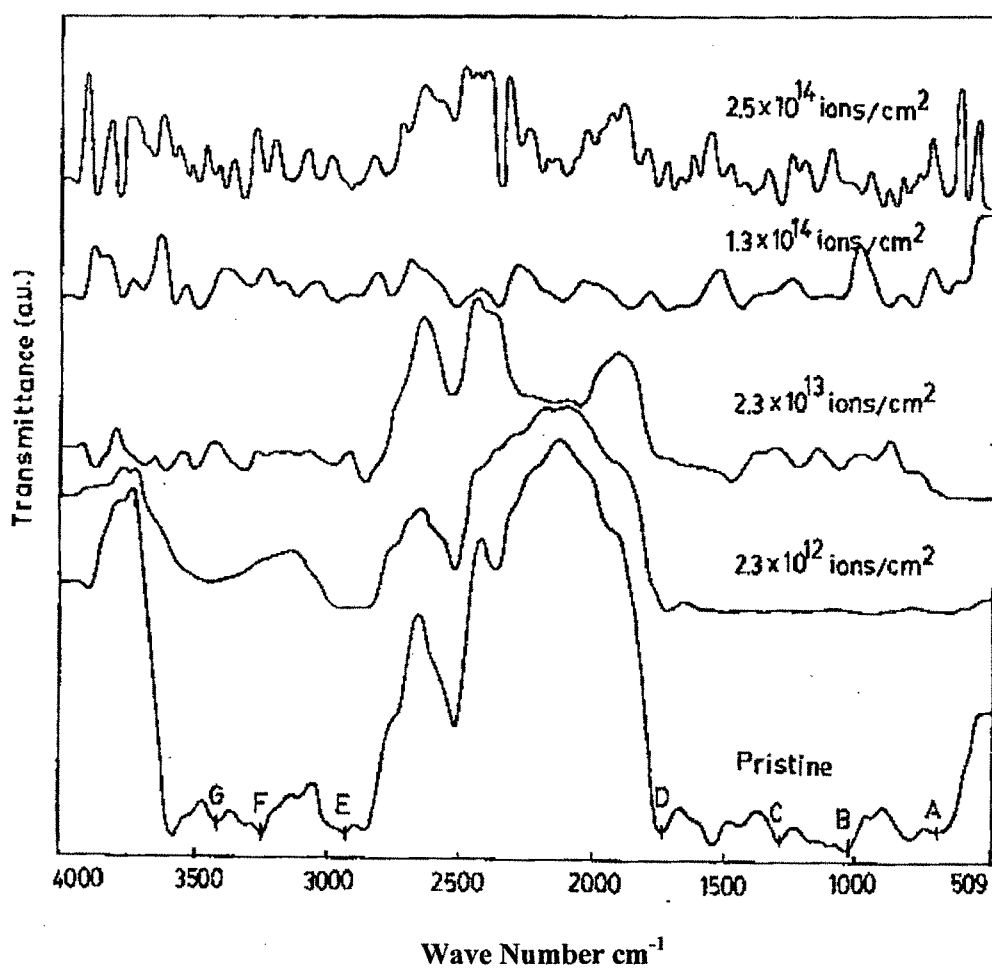

Figure 4.29 FTIR spectra of pristine and irradiated blended (PVC and PET) polymers.

4.4.2   Electrical Properties.

The electrical properties of pristine and irradiated polymeric blended (PVC + PET) films were measured using an LCR meter. The frequency was varied from 0.05 to 100 KHz, while the temperature was varied from ambient to 150°C respectively. Resistivity and conductivity were calculated using the formula given by equations (2.4) and (2.5) in article 2.3.1 (c) of chapter 2. The dielectric constant was calculated using the formula given by equation (2.9) in article 2.3.1 (d) of chapter 2. The findings with their respective explanation are as described below.

4.4.2 (a) log Resistivity v/s log Frequency.

Figure 4.30 shows plot of log resistivity v/s log frequency at different temperature keeping fluence constant. It is observed that the resistivity decreases rapidly in proportion to f^{-1}. The resistivity also decreases as the temperature increases. An ac field of sufficiently high frequency applied to a metal polymer metal structure may cause a net polarization, which is out of phase with the field. This results in ac conductivity, it appears at frequency greater than that at which traps are filled or emptied [6].

Figure 4.31 shows plot of log resistivity v/s log frequency for pristine and irradiated samples at ambient temperature. From the graph it can be seen that the resistivity of blended polymers decreases as frequency increases. It can also be seen that resistivity decreases with increase of fluence.
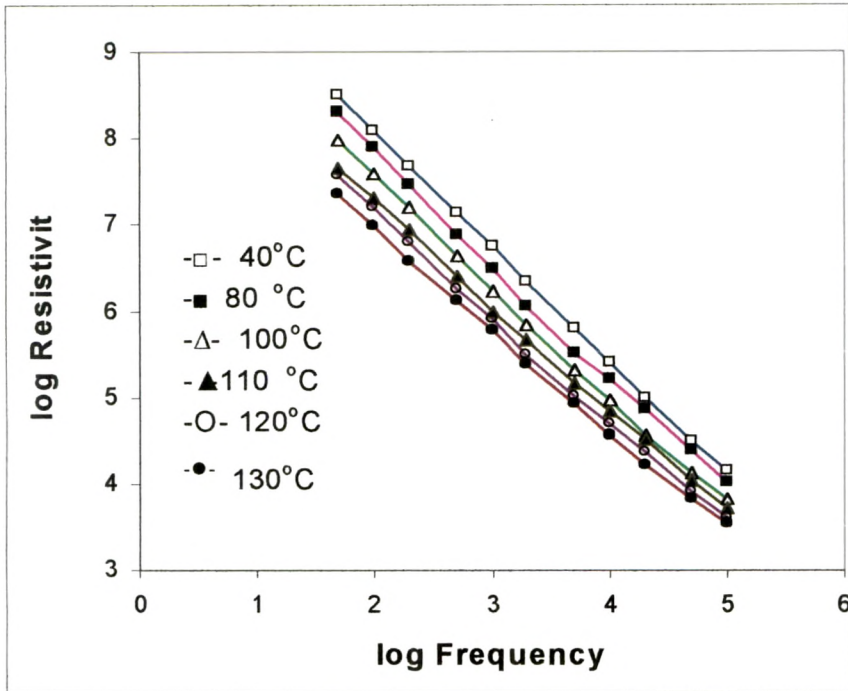
Figure 4.30   Plot of log Resistivity v/s log Frequency (f in Hz) at different Temperatures (^{o}C), keeping fluence (1.3 x 10^{14} ions/cm^{2}) constant.
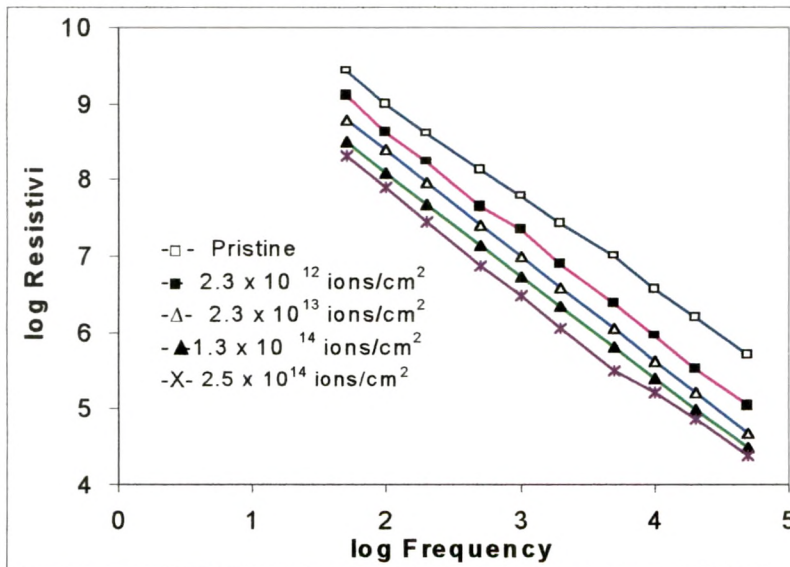

Figure 4.31   Plot of log Resistivity v/s log Frequency (f in Hz) at different fluence keeping temperature constant.

4.4.2 (b) Conductivity v/s log Frequency.

Figure 4.32 shows the dependence of conductivity on log frequency (f in Hz) at ambient temperature for pristine and irradiated samples. A sharp increase in conductivity has been observed at 20 kHz. It is also observed that conductivity increases as fluence increases. The increase in conductivity due to irradiation may be attributed to scission of polymeric chains and as a result increase of free radicals, unsaturation, etc. [6,7].

When an AC field of sufficiently high frequency is applied to a metal-polymer-metal structure, it may cause a net polarization, which is out of phase with the field. This results in AC conductivity, it appears at frequency greater than that at which traps are filled or emptied [6].
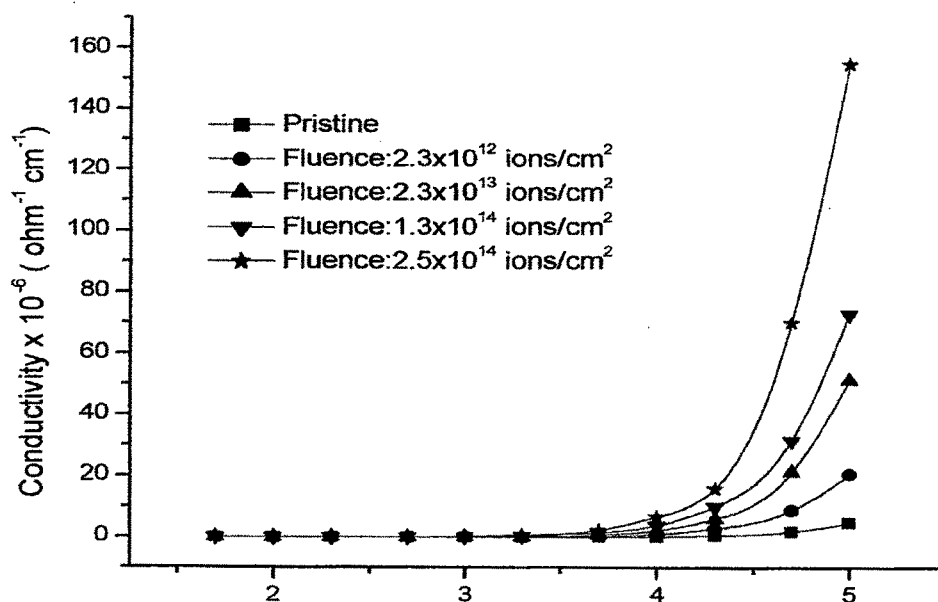

Figure 4.32   Plot of Conductivity v/s log Frequency (f in Hz) for pristine and

irradiated blended samples at ambient temperature.

4.4.2 (c)   tan δ v/s Temperature

Figure 4.33 shows the plot of dielectric loss v/s temperature at a frequency of 10 kHz

for pristine and irradiated samples. It is observed that dielectric loss increases with

increase in temperature. The dielectric loss is due to the perturbation of phonon system

by an electric field, the energy transferred to the phonon is dissipated in the form of

heat. The growth in tan δ and thus increase in conductivity is brought about by an

increase in conduction of residual current and the conduction of absorption current. The

small peak at $60^{\circ}C$ is due to the heat deflection temperature (HDT). In the amorphous

polymer, HDT is slightly $(10\text{-}20^{\circ}C)$ lower than T_g, whereas in semi-crystalline

polymers, HDT is more close to T_m. HDT is a useful indicator of the temperature limit

above which polymers cannot be used for structural (load- supporting) applications

[9] .The value of tan δ is also found to increase on increasing the fluence. This may be

attributed to scissioning of polymer chains and as a result of the increase of free

radicals, etc.

Figure 4.34 shows the variation of tan δ with temperature at different frequencies

keeping fluence constant. It is observed that loss factor (tan δ) increases as temperature

increases. It is also observed that tan δ increases as frequency increases. The dielectric

loss is due to the perturbation of phonon system by an electric field, the energy

transferred to the phonons is dissipated in the form of heat.
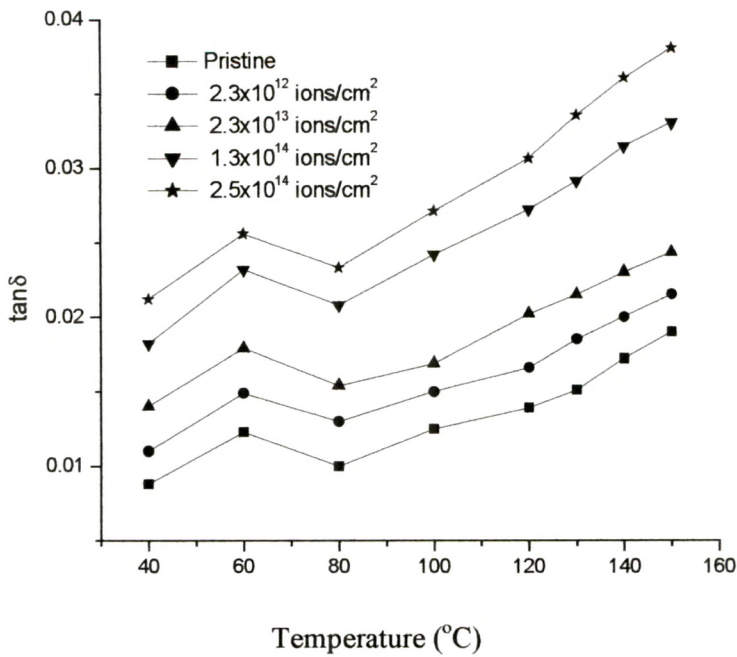
**Figure 4.33** Plot of Dissipation factor (tan δ) v/s Temperature (°C) at different fluence keeping frequency 10 kHz constant.
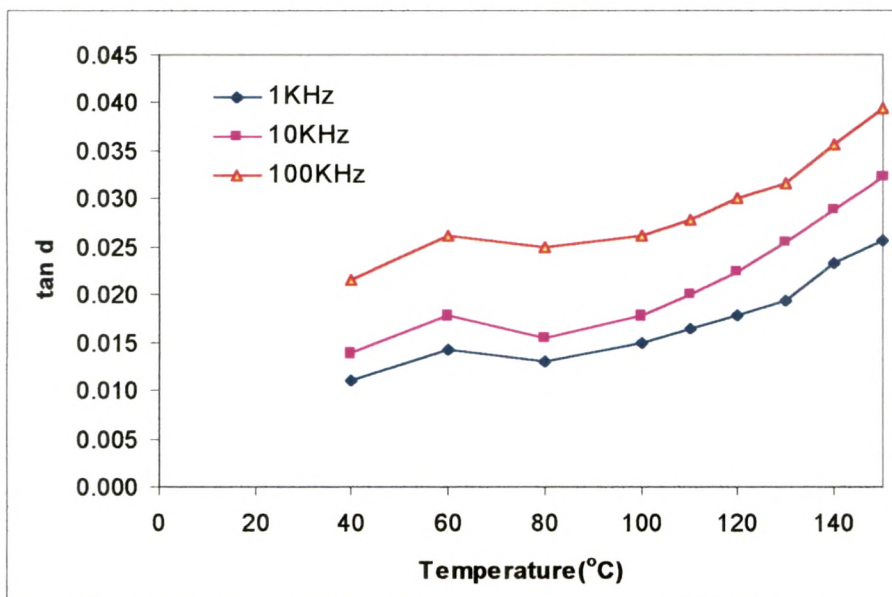
Figure 4.34 Plot of Dissipation factor (tan δ) v/s Temperature (°C) at different frequency keeping fluence (1.3 x 10^14 ions/cm^2) constant.

4.4.2 (d)   tan δ v/s log Frequency

Figure 4.35 shows the behaviour of tan δ as a function of log frequency at different temperatures keeping fluence constant (~1.3 x 10^{14} ions/cm^2). It is observed that with the increase of frequency, dielectric loss shows moderate increase at all temperatures.

Figure 4.36 shows the behaviour of tan δ measured as a function of log frequency for pristine and irradiated blended samples at ambient temperature. It is observed that loss factor increases moderately as frequency increases up to 10 kHz at all fluences. The growth in tan δ and thus increase in conductivity is brought about by an increase in the conduction of residual current and the conduction of absorption current [6,7].
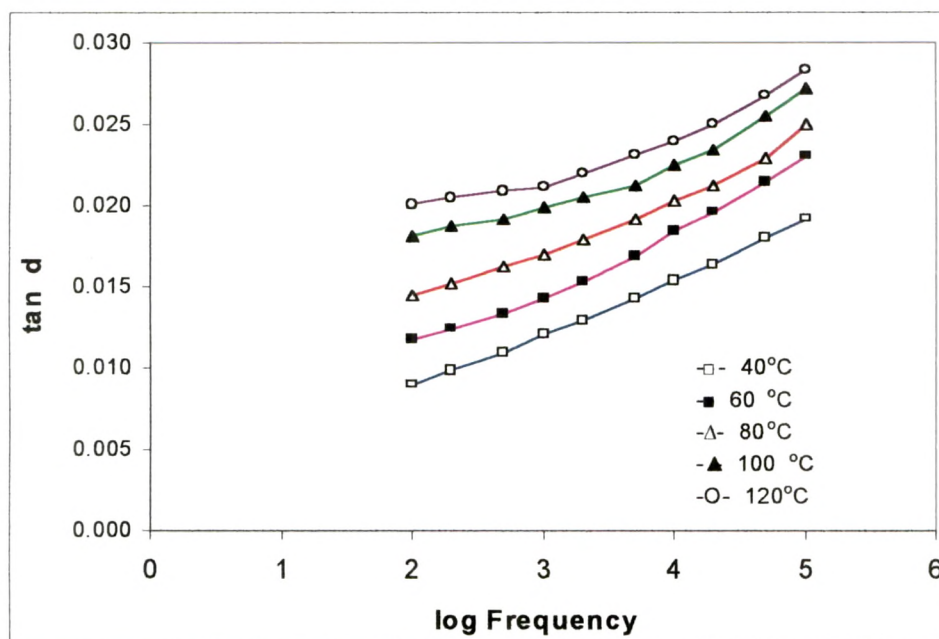
Figure 4.35   Plot of Dissipation factor (tan δ) v/s log Frequency (f in Hz) at different Temperature (°C) keeping fluence (1.3 x 10^{14} ions/cm^2) constant.
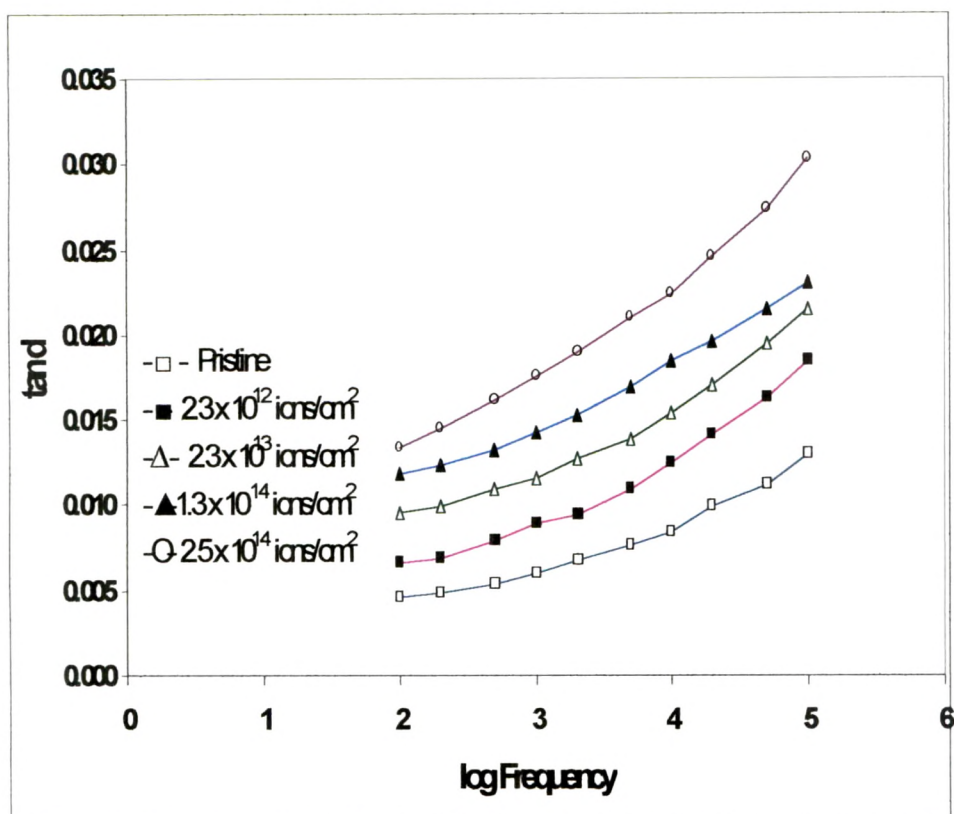
Figure 4.36 **Plot of Dissipation factor (tan δ) v/s log Frequency (f in Hz) for**

pristine and blended samples at ambient temperature.

4.4.2 (e) Dielectric Constant v/s log Frequency

Figure 4.37 shows the behaviour of dielectric constant as a function of log frequency at

different fluences. It is observed that the dielectric constant remains constant in the

frequency range 0.05 -100kHz. At these frequencies, the mobility of the charge carrier

is constant and thus the dielectric constant is constant. It is also observed that dielectric

constant increases as fluence increases. The increase in dielectric constant may be

attributed to chain scission and as a result the increase in the number of free radicals,

etc.
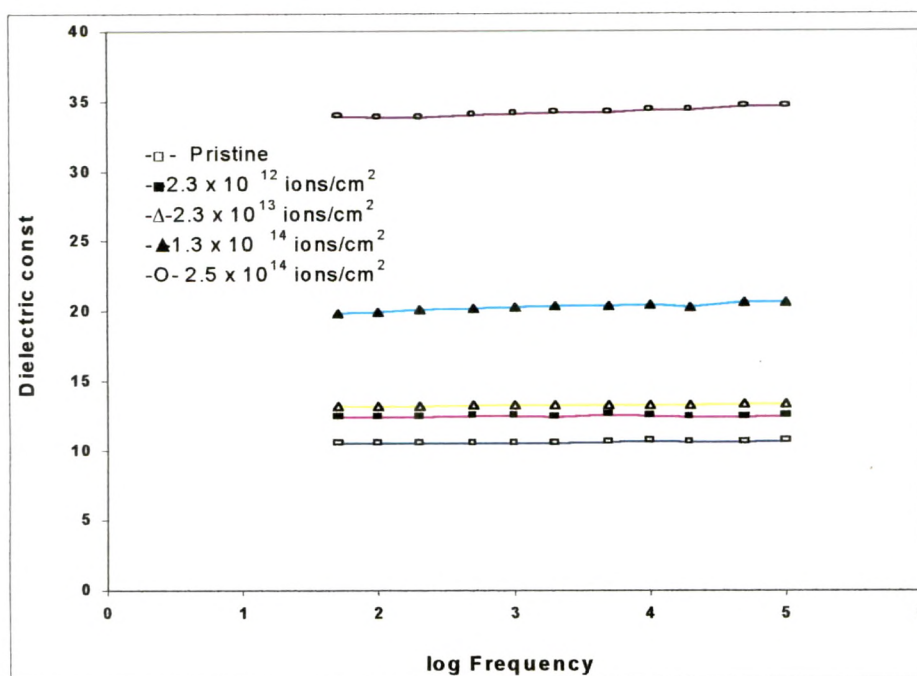
Figure 4.37 **Plot of Dielectric constant v/s log Frequency (f in Hz) at different fluences.**

4.4.2 (f) Dielectric Constant v/s Temperature

Figure 4.38 shows the dielectric constant as a function of temperature at 10 kHz for pristine and irradiated samples. Dielectric constant is almost constant with the increase in temperature. The negligible change (approximately 6%) in dielectric with temperature could be due to the effect of conductance corresponding to absorption current. It is also observed that the dielectric constant increases as fluence increases. This increase in dielectric constant may be attributed to chain scission and as a result an increase of free radicles, etc.
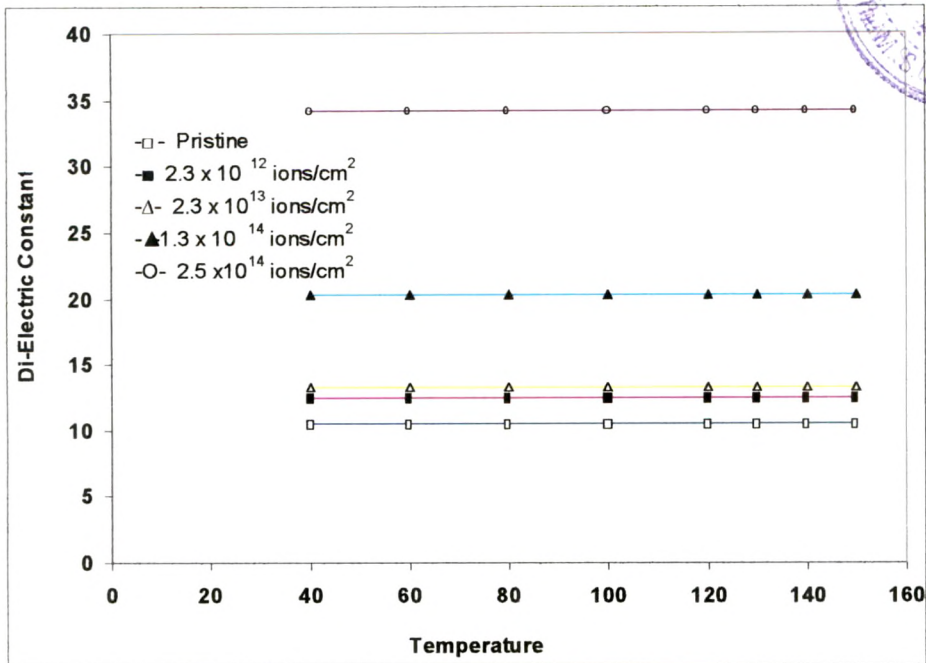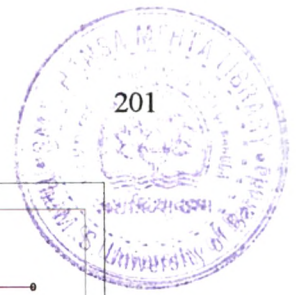
**Figure 4.38 Plot of Dielectric constant v/s Temperature (°C) at different fluences.**

4.4.3 Thermal Analysis of Blended (PVC + PET) polymer (Thermogravimetric analysis).

The decomposition behaviour of the pristine and the irradiated (1.3×10^{14} ions/cm^2) blended polymer was studied by this technique. The thermograms are as shown in the **Figure 4.41** and the temperature along with the respective weight loss (%) for different zones is given in **Table 4.3**. As seen in the figure the stable zone disappeared for the irradiated polymer, which was up to 170°C for pristine PVC + PET blended film. The slow decomposition zone was up to 260°C for pristine, which was up to 170°C for irradiated sample, involving only about 10% weight loss for the pristine, whereas a weight of about 12 % was lost in case of the irradiated sample.

Similarly, the fast decomposition zone went up to 310°C involving a weight loss of about 50 % for the pristine and up to 270 °C for the irradiated polymers associated with a similar amount of weight loss of 48 %. However the change observed was in the rate of decomposition. For the pristine sample, from 460°C to 500°C, fast decomposition was again observed, which was not there for irradiated sample. From the data, it is observed that the decomposition of irradiated (PVC + PET) blended polymer shows very little thermal stability and starts decomposing almost as soon as heat is supplied to it. It is also observed that the nature of the polymer decomposition depends on the fluence of ion beam, i.e. more the fluence, less the thermal stability. This denotes a degradation of the polymer matrix under Li^{3+} ion irradiation making it to decompose earlier than the pristine sample.
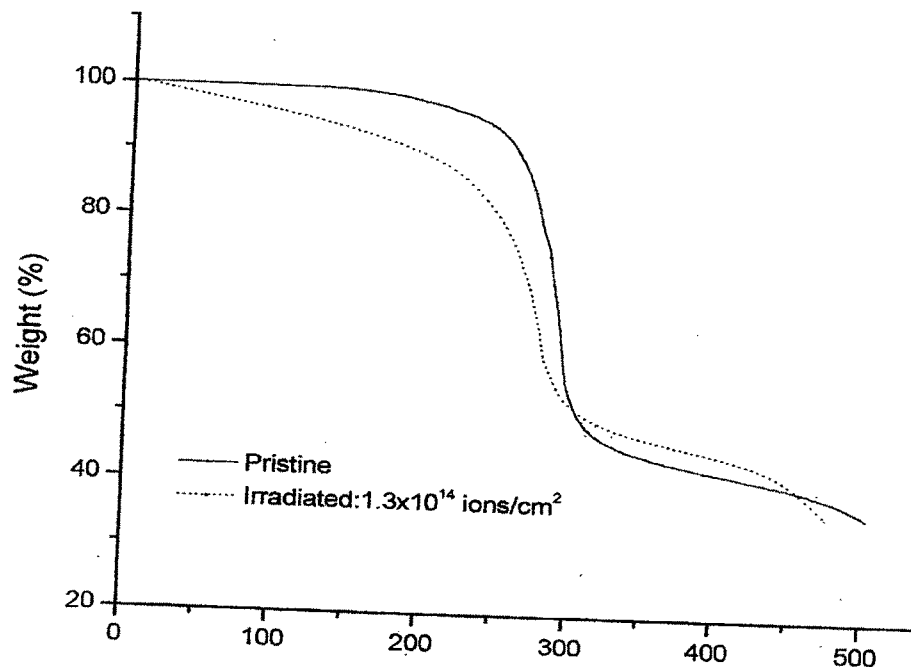
Figure 4.39   **Plot of TGA thermograms of pristine and irradiated**

(1.3 x 10^{14} ions/cm^2) blended PVC and PET

Table 4.3   Data derived from TGA thermogram of pristine and irradiated PVC + PET denoting their thermal decomposition behaviour.

Sample Weight (mg)	Zone	Temperature Range	Weight loss (%) in zone	Total Weight loss (%)	Interpretation
Pristine	I	0°C to 170°C	0	0	Stable Zone
	II	170°C to 260°C	10	10	Slow Decomposition
	III	260°C to 310°C	40	50	Fast Decomposition
	IV	310°C to 480°C	9	59	Slow Decomposition
	V	480°C o 500°C	7	65	Residue
Irradiated	I	0°C to 10°C	0	0	Stable Zone
	II	10°C to 170°C	12	12	Slow Decomposition
	III	170°C to 270°C	36	48	Fast Decomposition
	IV	270°C to 380°C	7	55	Slow Decomposition
	V	380°C to 500°C	20	75	Residue

4.4.4   Application of blended PVC and PET - <u>Gas Sensor</u>

A good sensor is supposed to have quick response. good repeatability, lower sensitivity. faster recovery time. longer life and must be economical. Gas sensors have several industrial applications, particularly hydrogen gas sensors. Hydrogen gas is characterized by its colourless, odorless and tasteless nature. It is hazardous and highly explosive in air atmosphere. Four volume percent of hydrogen in air is sufficient to

prove its hazardous nature. It requires low energy for ignition (≈ 0.02mJ). Hydrogen also has a rapid diffusion rate. The flame of hydrogen gas is invisible during the day time. Despite these safety disadvantages, hydrogen is a valuable component. Other hydrocarbon gases like ethane, methane, acetylene etc. pose similar problems [36-40].

Therefore, continuous sensing of hydrogen or hydrocarbon gases in atmosphere is of utmost importance from the safety point of view, particularly in industries like petrochemicals. Condition monitoring of electrical equipment e.g. power transformer is another important area where sensing of hydrogen is very significant. Dissolved gas analysis (DGA) of transformer coil is a well established popular and proven tool to monitor the health of power transformers in service. It can give indications of developments of incipient faults in transformer much earlier than any other protection device. There are several cases where DGA has saved a large number of transformers in service from premature failure. DGA is normally conducted annually on supposedly healthy transformers. Faults developed between two subsequent analysis cannot be detected. Therefore, on line sensing of gases has obvious advantages. It is found that sensing hydrogen alone is sufficient in detecting either type of fault, say thermal and electrical. Hydrogen gas sensors are commercially available in the market, but either they are very costly or not accurate.

On the other hand polymers are cheaper materials and it is reported that gas sensitivity of a polymer changes on exposure to high energy irradiation. In view of the above, an attempt has been made to explore the possibility of using a commercially available polymer, PVC blended with PET, after exposing it to high energy ion irradiation at different fluences, as a hydrogen gas sensitive material.

4.4.4(a) Experimental.

A polymeric chamber of dimension 95mm x 95mm x 80mm made up of PMMA sheet was fabricated and was kept at NTP. A schematic view of the experimental set up is shown in **Figure 4.40**. The chamber was equipped with two electrical feed through's, which hold the sample and a rubber port for injection of the hydrogen gas without leakage. A known quantity of hydrogen gas was injected into the chamber using a gas tight syringe and the electrical resistance of the film was measured. The concentration of hydrogen gas in the test chamber was measured by a Shimadzu, Japan make gas chromatograph. The surface resistance of four irradiated polymer and pristine sample were measured with the help of a Hewlett- Packard (model 4329A) high resistance meter.
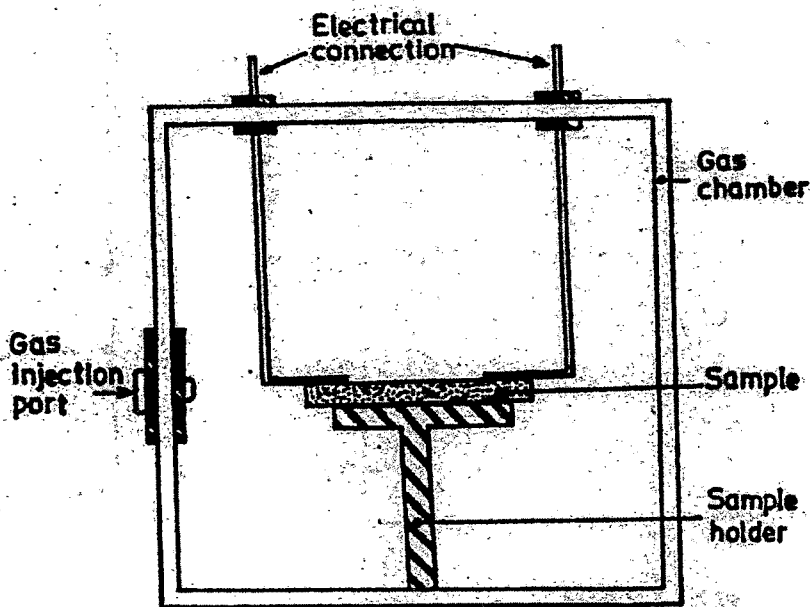
Figure 4.40 Schematic diagram of experimental set up for the study of gas sensor.

4.4.4(b) Results and Discussion.

The present work is aimed to develop an accurate and economical hydrogen gas sensor. The sensitivity range is chosen less than 1% due to its industrial requirement. Individual film was evaluated at a time, for hydrogen gas sensitivity in the test chamber. The results are shown in **Figure 4.41, 4.42 and 4.43** respectively.

It is inferred from **Figure 4.41** that electrical resistivity of the composite polymer decreases with the increase of ion fluence and is reduced to eight orders of magnitude (from 10^{15} Ω cm to 10^{7} Ω cm) due to ion irradiation. It is interesting to note that the resistivity of irradiated samples increases with the increase of concentration of hydrogen gas, where as pristine sample is unaffected by gas concentrations.

Figure 4.42 shows the variation of sensitivity with H_2 gas concentration at various fluences. Sensitivity is very small and almost constant at all concentration of H_2 gas at the fluence of 2.3×10^{12} ions/cm^2. It increases and becomes about 2.8 times at the fluence of 2.3×10^{13} ions /cm^2. Suddenly sensitivity increases more than 40 times at the fluence of 1.3×10^{14} ions /cm^2. But with further increase in the fluence to about 2.5×10^{14} ions/cm^2, the sensitivity decreased by a factor of about 3. This indicates that the ion dose of about 1.3×10^{14} ions / cm^2 is the optimum dose for sensitivity.

Figure 4.43 shows the variation of response time and recovery time with the fluence of ion beam for a small quantity of H_2 gas (0.05%). This indicates that the response time as well as the recovery time decreases as dose increases. Response time is defined as

the time needed to reach a maximum value of signal from the time of exposure to hydrogen gas. On the other hand recovery time is the time taken to come back to the original signal (base line) from the time of removal of hydrogen gas.
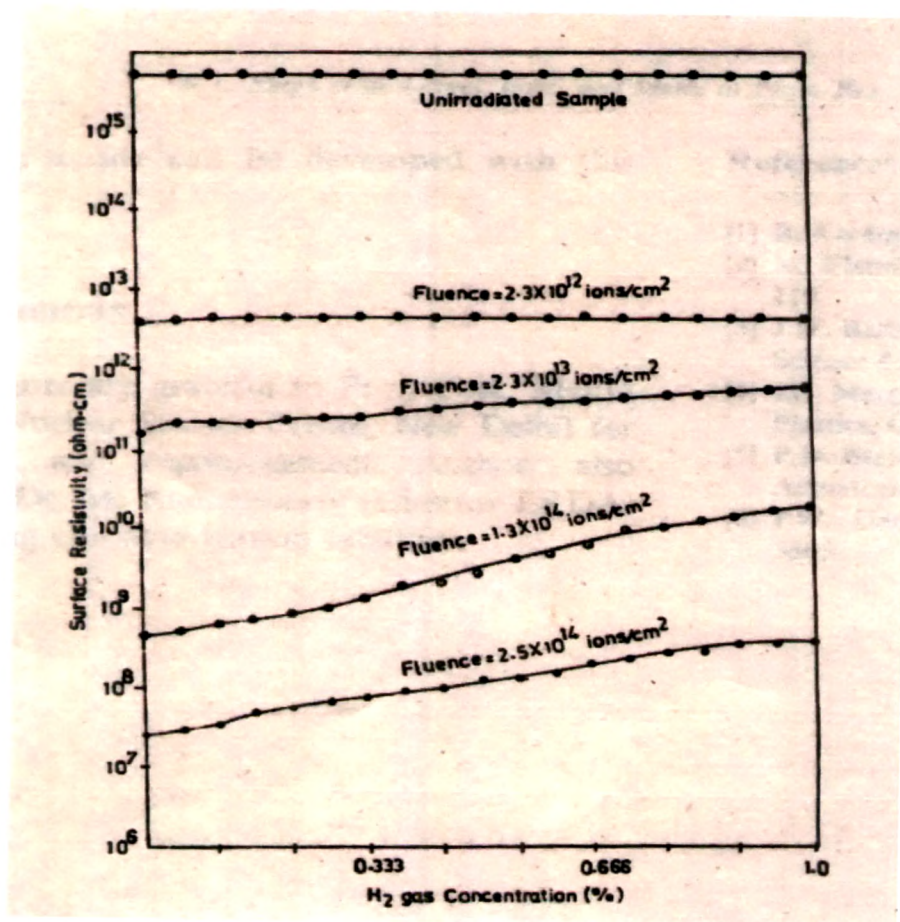

Figure 4.41   Plot of surface resistivity as a function of H_2 gas concentration at various fluences.
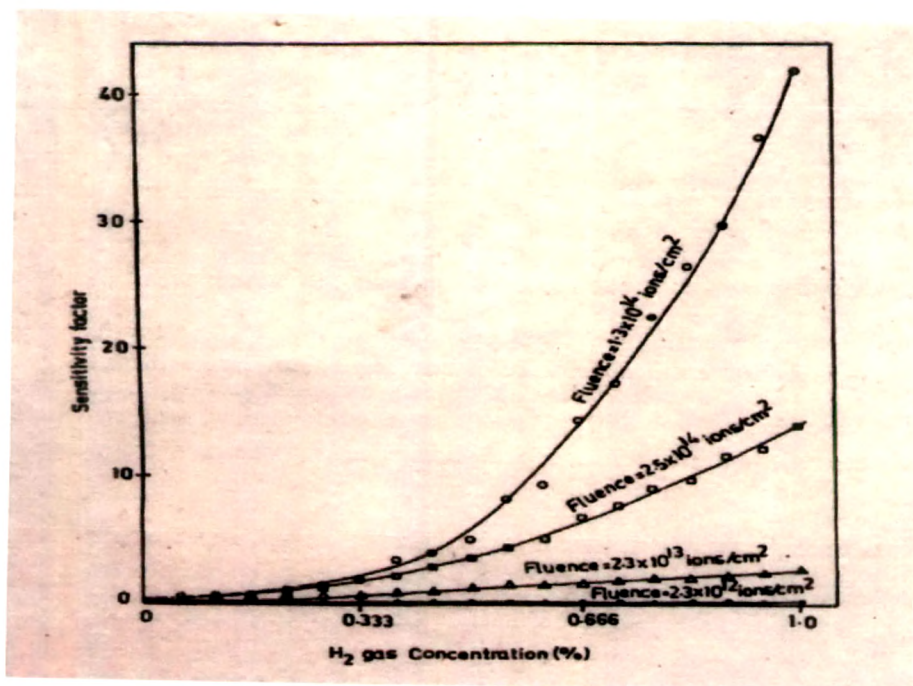
Figure 4.42   **Plot of sensitivity factor as a function of H_2 gas concentration at various fluences.**
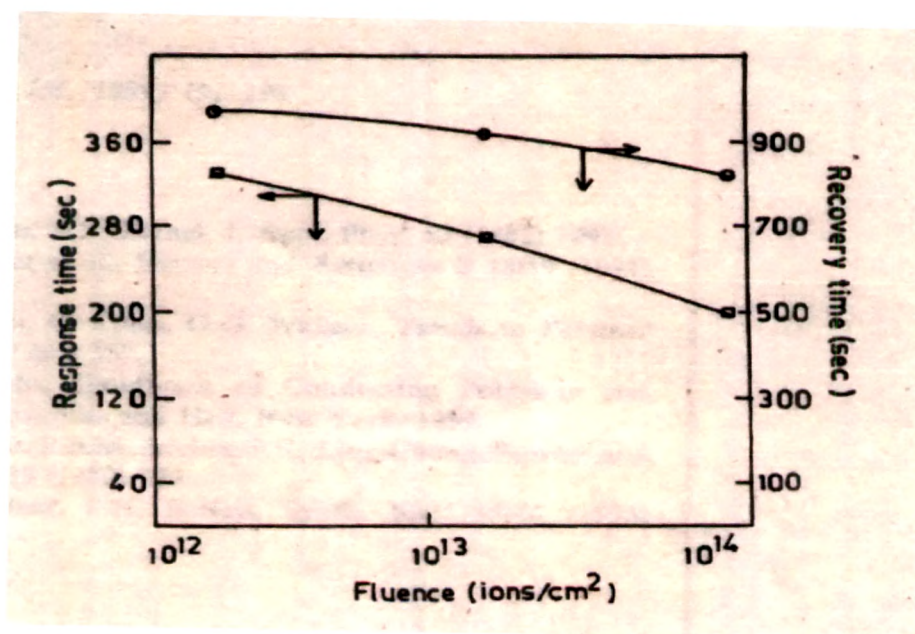

Figure 4.43 Plot of response and recovery times of irradiated polymers as a function of fluence for 500ppm of H_2 gas.

4.4.5   Conclusions

FTIR spectra of blended polymer before and after irradiation indicate that C-H, C-O-C, C=O molecular bands and groups which get modified or break down due to irradiation. It is found that the absorption bands characteristic of all functional groups decline, confirming their destruction by irradiation and they vanish gradually as irradiation proceeds. This might be attributed to breakage of chemical bonds and formation/emission of low molecule gases and radicals.

The ion irradiation of polymeric blends leads to chain scission and cross-linking and as a result there are changes in the dielectric properties. The growth in tan δ and thus increase in conductivity is brought about by an increase in the conduction of residual current and absorption current. The negligible change in dielectric with temperature could be due to conduction corresponding to absorption current. The loss factor shows a moderate increase up to 10 kHz frequency at all temperatures and fluences suggesting that this polymeric blend capacitor may be useful below 10 kHz frequency. The increase in dielectric loss/constant with fluence may be attributed to the increase of free radicals etc. due to irradiation.

From the TGA thermograms, it is observed that the decomposition of irradiated (at the fluence of 1.3 x 10^{14} ions/cm^2) blended polymer shows very little thermal stability and starts decomposing almost as soon as heat is supplied to it. It is also observed that the nature of the polymer decomposition depends on the fluence of the ion beam, i.e. more the fluence, less the thermal stability. This denotes a degradation of the polymer matrix under Li^{3+} ion irradiation making it to decompose earlier than the pristine sample.

The surface resistivity of irradiated polymer blends (PVC and PET) shows significant change with ion fluence. Ordinary polymer blend can be made sensitive to a gas by high energy ion irradiation. The sensitivity of the gas increases to about 40 times at an optimum radiation fluence of 1.3×10^{14} ions/cm^2. Various sensor characteristics response and recovery time, change in electrical resistivity due to exposure to hydrogen suggests that an economical and reliable sensor can be developed with this technique.

4.5   Blended Polymer (PVC + EVA)

As explained in the earlier topic 4.4 we are well aware of the need to make blended polymers. Polyvinylchloride (PVC) is one of the cheapest polymer which has very good electrical properties (i. e. tanδ, dielectric constant, electrical strength) where as Ethyl vinyl acetate (EVA) has an inherent flexibility and capacity to incorporate considerable amount of additives. The objective of the present work is to develop polymeric blend for industrial applications. Hence we studied the effects of high energy ions on its thermal and structural behaviors.

Polymer blends of poly vinyl chloride (PVC) and ethyl vinyl acetate (EVA) have been prepared as mentioned in chapter 3 (article 3.3.1) in different proportions of 30:70, 50:50 and 70:30, in two roll mill.

This study has been divided into two parts.

1. To study the mechanical and thermal properties of pure and polymeric blends of PVC and EVA using Instron Tensile Tester, (discussed in chapter 2, article 2.3.6) and Thermogravimetric analysis (discussed in chapter 2, article 2.3.7) respectively [42].

2. To study the change in the structural and thermal properties of pure and polymeric blend of PVC and EVC using FTIR spectroscopy and thermogravimetric analysis respectively at different fluences of 50 MeV Li^{3+} ions [43].

4.5.1 Mechanical Property of (Pristine) Pure and Blended Polymers.

Mechanical properties of the samples were measured as discussed in chapter 3 (article 3.35) using Instron Tensile Tester.

The load and elongation was automatically recorded on the chart. Every test shows breaking elongation and from the chart, the breaking load can be observed. From the load elongation curve, the yield point can be found out by Meredith's method [44]. Initially the instrument was set as shown in **Table 4.4** The charts are converted to a suitable form as shown in **Figure 4.44**. From the figure 4.44 breaking load, elongation and yield points were found out and tabulated as shown in **Table 4.5**.

The direct comparision of breaking load cannot be made as the thickness of the sample is not same. Therefore the relative terms breaking load per volume (BLPV) and yield load per volume (YLPV) are derived and then comparisons are made.

From **Table 4.5**, it is seen that the BLPV of PVC is much higher than EVA, while the polymeric blends show a higher value than EVA, but much lower than PVC. It can be said that PVC improved the strength of EVA, but on changing the proportion of PVC and EVA, the blend strength does not change much. But if the comparison is made on YLPV, the same effect was seen, but in this case the blend composition was affected. The maximum value was observed when PVC + EVA is (70:30) and the minimum, when it is (30:70). This indicates that the initial portion may have more interference by PVC, than by EVA. Comparison of the breaking elongation cannot be made as the thickness of the sample is not the same, but roughly it can be said that the blend breaking elongation lies between EVA and PVC, except for PVC + EVA (70:30).

Table 4.4   Sample's specification with instrument settings

| Sample	Cross Head speed Mm/min	Chart Speed Mm/min	Gauge Length mm	Sample width mm	Sample thickness mm	Sample volume mm^3
PVC+EVA(70:30)	10.0	10.0	10.0	1.0	0.28	2.8
PVC+EVA(50:50)	10.0	10.0	10.0	1.0	0.25	2.5
EVA	10.0	10.0	10.0	1.0	0.45	4.55
PVC	10.0	10.0	10.0	1.0	0.15	1.5
PVC/EVA(30:70)	10.0	10.0	10.0	1.0	0.37	3.75
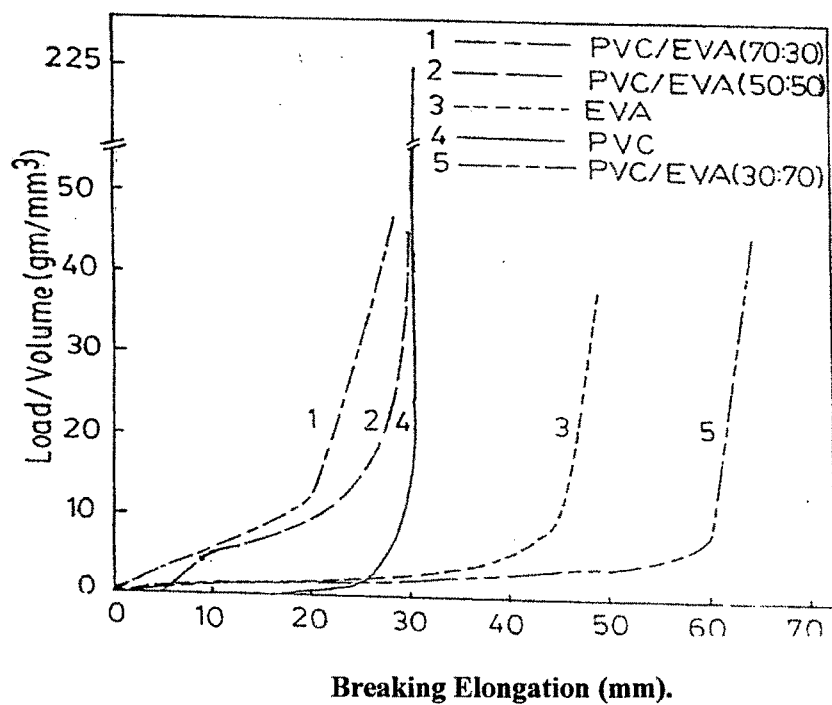
Figure 4.44 Load – elongation curves.

Table 4.5 . Mechanical properties of the samples.

Sample	Breaking load (g)	Breaking load per volume (BLPV) (g/mm^3)	Breaking elongation (mm)	Yield load (g)	Yield load per volume (YLPV) g/mm^3	Yield elongation (mm)
PVC+EVA(70:30)	131.0	46.79	29.0	24.0	8.57	15.95
PVC+EVA(50:50)	114.0	45.60	32.5	17.68	7.07	200.83
EVA	175.0	38.46	48.0	21.53	4.73	153.02
PVC	335.0	223.33	30.9	12.88	8.58	27.38
PVC+EVA(30:70)	170.0	45.33	63.0	21.76	5.80	30.68

4.5.2   Structural Analysis of Irradiated, Pure and Blended Polymers.

To study the structural changes including the alteration in positions and intensity of the characteristic bands, the FTIR spectroscopy of all samples were recorded in the wave numbers range of 4000-500 cm^{-1}.

The IR absorption spectrum of each sample was examined before and after the irradiation. The FTIR spectra of pristine and irradiated (at the fluence of 10^{14} ions/cm^2) pure and blended samples are shown in **Figure 4.46**. We select the absorption bands as (A) 600-800 cm^{-1}: C-Cl stretching vibration , C-H bending vibration; (B) 1730 cm^{-1} : C=O stretching vibration;(C) 2916 cm^{-1} : C-H stretching vibration; (D) 3400-3700 cm^{-1}: O-H stretching vibration for analysis, since they have a relatively large absorbance. It is observed that integrated absorbance of all four functional groups decline, confirming scissioning of polymer chains due to ion beam irradiation. There is a significant change in the overall structure of the polymers.
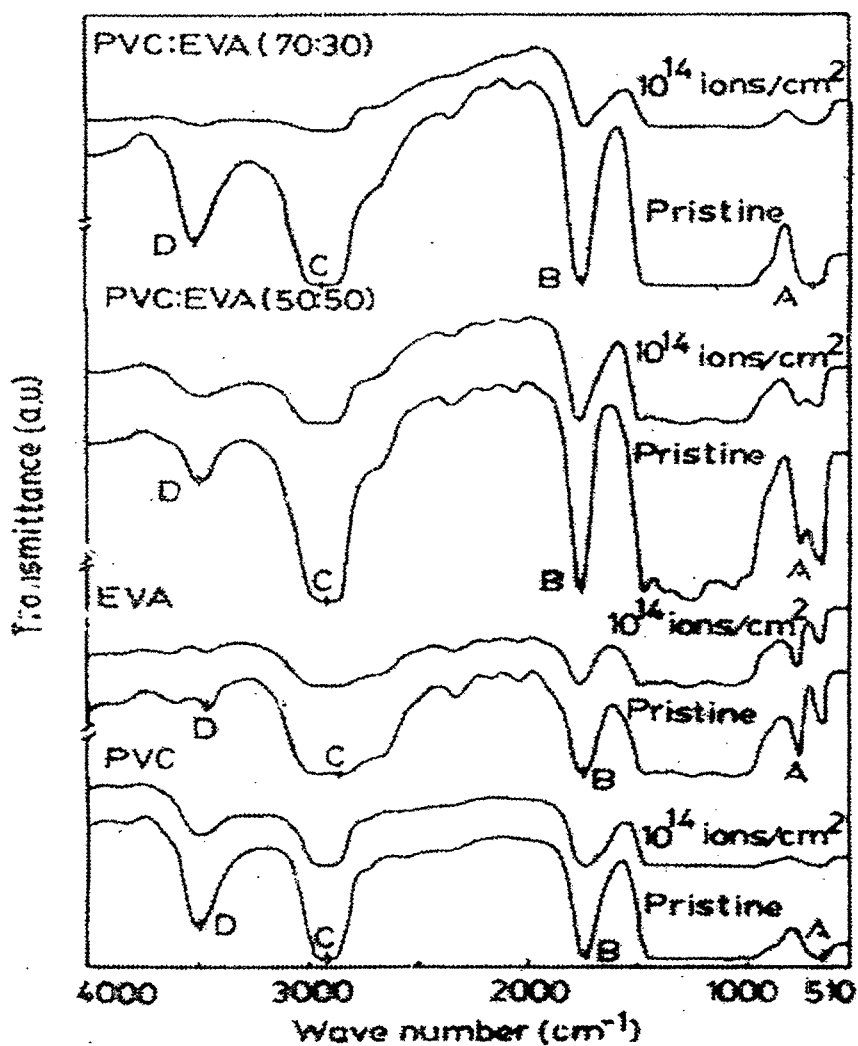
Figure 4.45 FTIR spectra of pure and blended pristine and irradiated samples.

4.5.3 Thermal Analysis of Pristine, Pure and Blended Polymers.

The TGA thermograms of pure and blended PVC and EVA are shown in **Figure 4.45**.

It is quite evident from thermograms that there is an increase in the thermal stability of

PVC due to incorporation of EVA in equal proportion by weight. TGA analysis revealed a two step decomposition pattern for blended polymers while pure polymer exhibits single step decomposition [9].The weight loss (%) with the temperature for different polymers is listed in **Table 4.6.** As depicted from the figure 4.45, pure PVC remains stable up to 110°C where there is no weight loss of the sample.

This stable zone is followed by a slow rate of decomposition from 110°C to 230°C. A fast rate of decomposition starts after that till the sample is roughly decomposed by about 77% at 280°C. At temperatures above 280°C, bulk decomposition of the polymer residue took place while pure EVA exhibits a stable zone up to 130°C where there is no weight loss. The stable zone is followed by the slow rate of decomposition from 130°C to 410°C and then a fast rate of decomposition started till the sample roughly decomposed by about 92% at the temperature of 440°C. The nature of the thermograms of polymeric blend is different compared to pure samples. Blended PVC and EVA (50:50) is stable up to about 130°C. A slow rate of decomposition took place from 130°C to 200°C where the sample losses about 6% of initial weight. This zone is followed by a fast rate of decomposition from 200°C to 290°C with a weight loss of 6 to 31%. There is further slow decomposition from 290°C to 400°C with a weight loss of 31 to 43%, after that the fast decomposition took place from 400°C to 460°C where a weight loss of about 43 to 79% of the initial weight took place.

In the case of PVC and EVA (70:30) the stable zone is observed up to 110°C. The slow rate of decomposition started from 110°C to 250°C where the weight loss of about 0 to

29% of the initial weight took place. This zone is followed by a fast rate of decomposition from 250°C to 330°C with a weight loss of 29 to 57%. This is further followed by a slow rate of decomposition from 330°C to 460°C with a weight loss of 57 to 73% of the initial weight.

Thus it is observed that the thermal stability of PVC increased by incorporating EVA in equal composition.
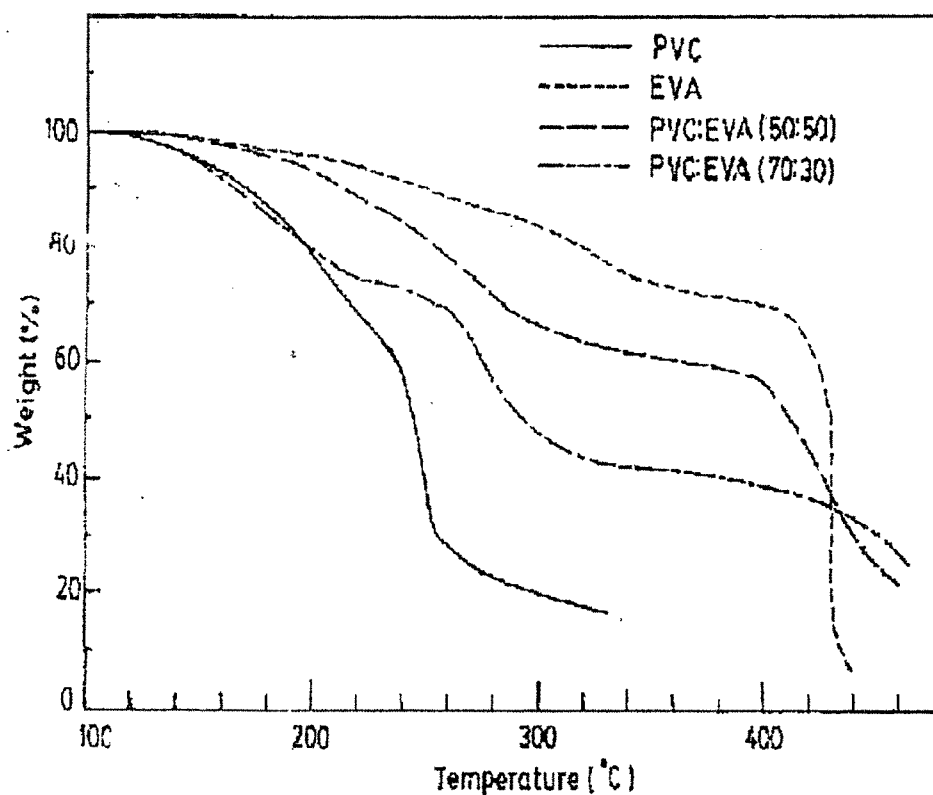
Figure 4.46 TGA thermograms of pristine PVC, EVA and their blends.

Table 4.6   Thermal decomposition temperatures at different zones for PVC, EVA and their blend.

Sample	Zone	Temperature	Weight loss (%)	Interpretation
PVC	I	0°C to 110°C	0	Stable
	II	110°C to 230°C	0-35	Slow decomposition
	III	230°C to 280°C	35-77	Fast decomposition
	IV	280°C to 330°C	77-82	Residue
EVA	I	0°C to 130°C	0	Stable
	II	130°C to 410°C	0-32	Slow decomposition
	III	410°C to 440°C	32-92	Fast decomposition
PVC+EVA (50:50)	I	0°C to 130°C	0	Stable
	II	130°C to 200°C	0-6	Slow decomposition
	III	200°C to 290°C	6-31	Fast decomposition
	IV	290°C to 400°C	21-43	Slow decomposition
	V	400°C to 460°C	43-79	Fast decomposition
PVC+EVA (70:30)	I	0°C to 110°C	0	Stable
	II	110°C to 250°C	0-29	Slow decomposition
	III	250°C to 330°C	29-57	Fast decomposition
	IV	330°C to 460°C	57-73	Slow decomposition

4.5.4   Thermal Analysis of Irradiated, Pure and Blended Polymers.

The TGA thermograms of pristine and irradiated (fluence 10^{14} ions/cm^2) pure and

blended PVC and EVA are shown in **Figure 4.47**. It is quite evident from the

thermograms that there is an increase in the thermal stability of PVC due to

incorporation of EVA in equal composition by weight. It is also revealed the blended

polymer shows double step decomposition while pure polymer exhibits single step

decomposition. The stable zone of pristine and irradiated samples is shown in **Table**

4.7. It is quite evident from the thermograms that there is a decrease in the thermal

stability due to irradiation. In each case, the stable zone is followed by a slow rate of

decomposition and then a fast rate of decomposition. Thus it is concluded that the

thermal stability of PVC increased by incorporating EVA in equal composition. This

fact is also observed from the pristine, pure and blended polymers (Figure 4.45).
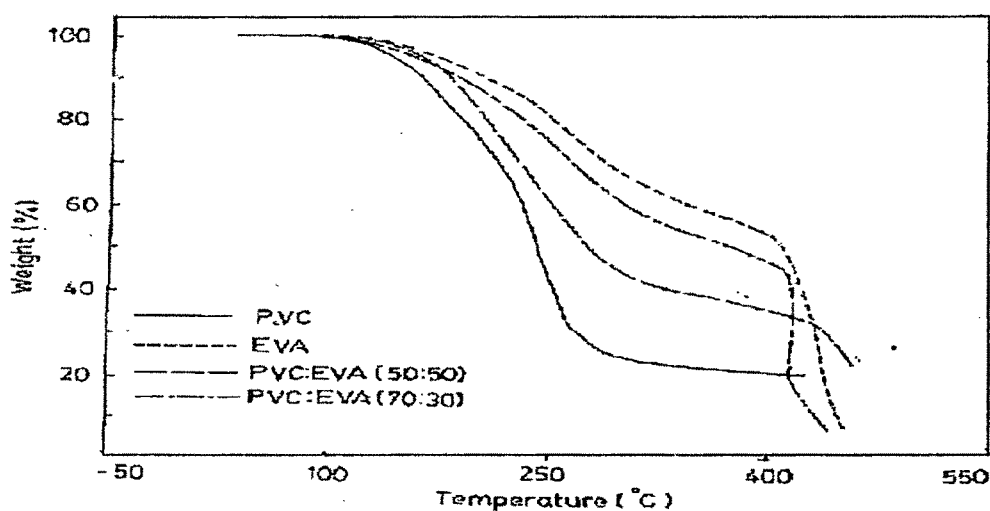
Figure 4.47 TGA thermograms of pristine PVC, EVA and their blends irradiated

at 10^{14} ions/cm^2.

Table 4.7 **Thermal decomposition temperatures of pristine and irradiated samples.**

Samples	Stable zone temperature (^{0}C)		Remarks
	Pristine sample	Irradiated sample $(10^{14}$ions/ cm$^2)$	Stable zone(0% weight loss) followed by slow and then fast decomposition zones.
PVC	110	93	
EVA	130	119	
PVC+EVA(50:50)	130	115	
PVC+EVA (70:30)	110	100	

4.5.5   Conclusions.

From the study of pristine and blended samples of PVC and EVA following conclusions can be drawn.

1   The mechanical strength of EVA improved by adding PVC.

2   The yield strength of blend improved gradually by blending PVC with EVA.

3   It is evident that due to blending the thermal properties of PVC have increased and have become almost comparable to EVA.

4   Elongation cannot be compared as the thickness of the polymer was not the same and for better comparison the samples are required in circular filament type form.

5   The blend consisting of PVC and EVA in equal proportion (50:50) exhibits better thermal property among all, indicating its possible industrial applications.

6   It is observed from the comparison of FTIR spectra of pristine and irradiated pure and blended polymers that the intensity of the functional groups are observed to

change on irradiation fluence. This may be attributed to breakage of polymer chains.

7   It is evident from TGA thermograms that the degradation of polymer matrix occurs under Li-ion irradiation and makes it to start decomposing earlier than the pristine sample in all cases.

REFERENCES

1. G. H. Wang, G. Q. Pan, L. Dou, S. T J.Zhang, L.Q. Dai, Nucl. Instru. and Meth. 27 (1987) 410.

2. R. Mishra, S.P.Tripathy, D. Sinha, K.K.Dwevedi, S.Ghosh, D.T.Khathing, M.Muller, D.Flink, W. H. Chung. Nucl. Inst. and Meth. B 168 (2000) 59.

3. R. Mishra, S.P.Tripathy, K.K.Dwevedi, D.T.Khathing, S.Ghosh, M.Muller, D.Flink, Radiation Measurements 33 (2001) 845.

4. N.L. Singh, Anita Sharma, V. Shrinet, A. K. Rakshit and D.K. Avasthi, The 5th IUMRS International Conference in Asia, Bangalore, India, October 13-16, 1998.

5. N. L. Singh, A. Sharma, V. Shrinet, A. K. Rakshit and D. K. Avasthi, Bull. Mater. Sci., 27 (2004) 263.

6. A. K. Jonscher, Nature 267,(1977) 673.

7. N.P. Bogoroditsky, V.V. Pasynkov and B. M. Tareer, Electrical Engineering Materials, Mir Publications, Mosow, 1979.

8. M. C. Wintergill and J.J. Fontanella, Polymer electrolyte review (eds), H J R Mc Callum and C A Vincent (London: Elsevier Applied Science) Vol.2, 1989,43.

9. J. R. Fried, Polymer science and technology (New Delhi: Prentice Hall of India Pvt Ltd) 2000, 155.

10. Idem,Thin Solid Films 113 (1984)331

11. M. Mujahid, S. Gupta, D. K. Avasthi and D.S. Srivastava, Proceedings of the Solid State Physics, Symposium 42 (1999) 599.

12. K.Ciesla, W.Starosta, Nucl. Instr. and Meth. B 105 (1995) 115-119

13. T. Steckenreiter, E. Balanzat, H. Fuess, C. Trautmann, Nucl. Instr. and Meth.B 131 (1997) 159-166.

14. A. Biswas, S. Lotha, D. Fink, J.P. Singh, D.K. Avasthi, B.K. Yadav, S.K. Bose, D.T. Khating, A.M. Avasthi, Nucl. Instr. and Meth. B 159 (1999) 40-51.

15. S.P. Tripathy, R. Mishra, K.K. Dwivedi, D.T. Khathing, S. Ghosh, D. Fink Radiation Measurements 36 (2003) 107-110.

16. B. Bridwell, R.E. Giedd, Y.Q. Wang, S.S. Mohite, T. Jahnke, Nucl. Inst. and Meth. B 56/57 (1991) 656.

17. K. Ueno, Y. Matsumoto, Nucl. Instr. and Meth. B 59/60 (1991)1263.

18. P. H. Soni, Anita Sharma, N.L. Singh, C.F. Desai, N. R. Shah, V. Shrinet and D. K. Avasthi, Annual Report, Nuclear Science Centre, New Delhi, (1999-2000) p 109.

19. N.L.Singh, A. Sharma, D. K. Avasthi, Nucl. Instr. and Meth. B 206 (2003) 1120.

20. Anita Sharma, Anjum Qureshi, N.L.Singh, D.K.Avasthi and V. Shrinet, Solid State Physics symposium, Dec.26-30, 2004,G.N.D Univ. Amritsar.

21. T.G. Fox and P.J. Flory , J.Am. Chem. Soc.70(1948)2784

22. G.E. Roberts, and E.T.F. White, In the Physics of Glossy polymers, R.N.Haward (Ed.), Applied Science Publishers, London (1973) pp 179

23. E.H.Lee, G.R.Rao,L.K.Mansar, Mater. Sci., Forum, 248-249 91997) 135.

24. V.Shrinet, U.K.Chaturvedi, S.K.Agarwal, Vakil Singh and A.K.Nigam, Nucl. Inst. and Meth. 209/210 (1983) 1193-1199.

25. D. Xu, X.L. Xu, G.D.Du, R. Wang, S.C. Zou, and X.H. Liu, Nucl. Inst. and Meth. B80/81,1993, 1063.

26. D. Fink, F. Hosoi, H. Omichi, T. Sasuga, L. Amaral, Rad. Eff. Defects in Solids 132, 1994, 313.

27. T. Kobayashi, Takayuki Terai, Nucl. Instr. and Meth. B 166-167 (2000) 627.

28. H.S. Virk, P.S. Chandi, A.K. Shrivastava, , Bull. Mater. Sci., 2001, 24,2001, 529.

29. R. Mishra, S.P. Tripathy, K.K. Dwevedi, D.T.Khathing, S.Ghosh, M.Muller, D.Flink, Radiation Measurements 36 (2003) 639.

30. R. Mishra, S.P. Tripathy, K.K. Dwivedi, D.T. Khathing, S. Gosh, M. Mueller, D. Flink, Rad. Measurements 36 (2003) 621.

31. Anita Sharma, N.L. Singh, M.S.Gadkari, V. Shrinet and D.K.Avasthi, The 5th IUMRS International Conference in Asia, Bangalore, India, Oct. 13-16,1998.

32. A. Sharma, N.L.Singh, M.S.Gadhari, V. Shrinet, D.K.Avasthi, J. Macro Mole. Sci PAC A 42 (2005) 149.

33. G. Gittus, Irradiation effects in solids. Appl. Sci., London. 1978, 484.

34. R.D.S. Yadav, N.I. Singh, A.K.Nigam, V. Singh, J. Nucl. Mater. 102 (1981), 109

35. S.K. Avasthi, R. Bajpai, Indian J. Pure and Applied Physics,39,2001 795.

36. B. Keramati, Z. N. Zernel, J. Appl. Phys. 52 (1982) 1091.

37. M. Fleischer et al. Sensors and Actuators B 18/19 (1994) 119.

38. J. N. Barisci, C. Conn, G. G. Wallace, Trends in Polymer Science 4 (1996) 307.

39. M. Margolis, Handbook of Conducting Polymers and Plastics, Chapman and Hall, New York, 1989.

40. P. N. Barlett, P.B.M. Archer, S.K.Ling-Chung, Sensors and Actuators 19 (1989) 125.

41. J.W. Gardner, P. N. Barlett, Synth. Met. 55-57 (1993) 3665.

42. A. Sharma, A. Qureshi, M.S. Gadkari, N. L. Singh, S.Bhattacharya and V. Shrinet, National Seminar on "Polymers and Applications", NITTTR, Chandigarh, India, Feb 5-7, 2004. Communicated to J. of Eng. and Mater. Sci.

43. Anita Sharma, Anjum Qureshi, N.L.Singh, V.Shrinet, D.K.Avasthi and A.K.Rakshit, National Seminar on Polymers, Surfactants and Gels, Department of Chemistry, M. S.U. Baroda, March 11-13, 2005. Communicated to Ind. J. Pure and Applied Phys.

44. R. Meredith, J. Text. Inst. 36 (1945) T 107; 37 (1946) 469.